Electronic Supplementary Material (ESI) for Journal of Materials Chemistry C.

Supporting Information

Critical analysis of self-doping and water-soluble n-type organic semiconductors: structures and mechanisms

Lewis M. Cowen, Peter A. Gilhooly-Finn, Alexander Giovannitti, Garrett LeCroy, Harry Demetriou, William Neal, Yifan Dong, Megan Westwood, Sally Luong, Oliver Fenwick, Alberto Salleo, Sandrine Heutz, Christian B. Nielsen, and Bob C. Schroeder

Contents

General Experimental Procedures

Commercially available compounds and solvents were used as received. Solution NMR spectra were recorded using a Bruker Avance III 400 and Neo 700 spectrometer, operating at 400 and 700 MHz, respectively. Chemical shifts are reported in ppm with the residual solvent peak of $CHCl_3$ (δ = 7.26 ppm, s) DMSO (δ = 2.50 ppm, s) or H_2O (δ = 4.79 ppm, s) as the internal standard for ^1H NMR. UV-Vis spectra were recorded in aqueous solutions or thin-films on glass substrates on a Shimadzu UV-2600 or Shimadzu UV-3600i Plus UV-VIS-NIR spectrophotometer. Glass substrates for UV-vis were prepared by sonicating in soapy deionised water, acetone and IPA consecutively for 15 mins each. Thin-films were drop-cast onto glass substrates from 5 mg/mL, 2.5 mg/mL or 0.5 mg/mL solutions from aqueous solutions. Fourier Transform Infrared (FTIR) spectroscopy was recorded on a Shimadzu IRTracer-100 with an attenuated total reflectance (ATR) setup. High resolution mass spectrometry (HRMS) with electrospray ionisation (ESI) was performed via direct injection on a Thermo Orbitrap Exactive Plus Mass Spectrometer. Atomic force microscopy was carried out in tapping mode on a Bruker Dimension® Icon™ Scanning Probe Microscope. X-ray fluorescence was carried out under an inert nitrogen atmosphere with a Malvern Panalytical Epsilon 4 spectrometer equipped with a silver (Ag) anode X-ray tube.

Cyclic voltammetry (CV) was performed on an Autolab/PGSTAT101 potentiostat in 0.3 M aqueous solutions of potassium chloride as electrolyte. Glassy carbon was used as working electrode, a platinum wire as counter electrode and silver/silver chloride (Ag/Ag^+) as reference electrode. The LUMO energy levels were then estimated according to the equations EA (eV) = 4.71 + E_{onset} where E_{onset} is the onset of reduction or EA (eV) = 4.71 + $E_{1/2}$ where $E_{1/2}$ is the half potential of reduction.[1-3]

Glass substrates used for EPR were sonicated with deionised water, acetone and IPA consecutively before 10 µL of a 5 mg/mL aqueous solution of NDI-NMe_3Br or NDI-OH was drop-cast. Measurements were conducted at room temperature using a Bruker ELEXSYS-II E580 EPR spectrometer, with a Bruker ER4118-X MD5 resonator operating in continuous wave (CW) mode at X-band. The following experimental parameters were used for all measurements: modulation frequency = 100 kHz, modulation amplitude = 1 G, attenuation = 20 dB. Spectra were produced and analysis performed using the EasySpin simulation toolbox (release 5.2.33) with MATLAB 2017b.[4]

For the conductivity measurements, glass slides (1 × 1 cm) were cleaned with soapy water, deionised water, acetone and then IPA by sonication for 15 minutes in each solvent. This was followed by O_2 plasma cleaning for 30 minutes using a Harrick Plasma PDC-32C. 100 µL of the 5 mg/mL NDI-OH aqueous solutions were drop cast onto the clean glass slides at the specific drop-cast temperature and covered with a glass petri dish. Once the slides were visibly dry they were kept under vacuum prior to measurements. Thickness of films was measured with a Dektak 3ST surface profiler. Conductivity was then measured in air using a Keithley 4200 semiconductor characterisation system. Using four probes, contacted directly onto the film with no electrodes, in a Van der Pauw geometry, the horizontal and vertical resistances, R_h and R_v, were measured and related to the sheet resistance, R_s, using equation:

$$e^{\frac{-\pi R_h}{R_s}} + e^{\frac{-\pi R_v}{R_s}} = 1 \qquad \text{(eq 1)}$$

With a known thickness of thin-film, t, the resistivity, ρ, could then be calculated and related to the conductivity, σ, using the two equations below:

$$\rho = R_s \times t \qquad \text{(eq 2)}$$

$$\sigma = \frac{1}{\rho} \qquad \text{(eq 3)}$$

Synthetic Procedures

NDI-TEG was synthesised using the procedure reported by De et al.[5]

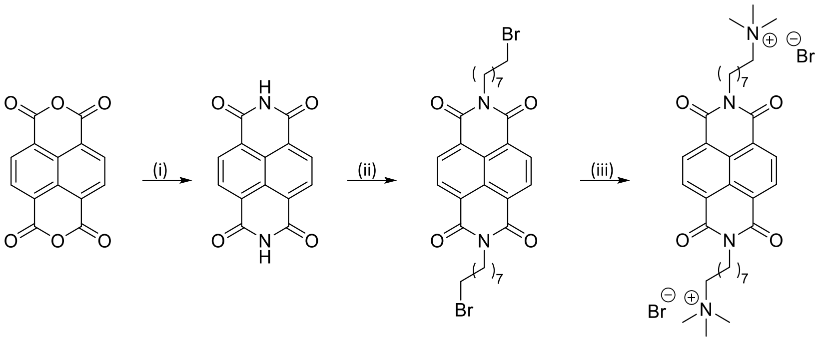

1 2 3 **NDI-NMe$_3$Br**

Scheme S1. *Synthesis of NDI-NMe$_3$Br. Reagents and conditions: (i) NH_4OAc, AcOH, reflux 1 h. (ii) 8-bromooctan-1-ol, DEAD, PPh_3, THF, 14 h. (iii) $NMe_3{\cdot}HCl$, $NaHCO_3$, MeCN, 80 °C, 12 h.*

1,4,5,8-Naphthanlenetetracarboxylic diimide (2)

Adapted from a previous report [6], naphthalenetetracarboxylate dianhydride (1) (8.00 g, 0.0300 mol) and ammonium acetate (46.25 g, 0.600 mol) were suspended in acetic acid (200 mL). The orange reaction mixture was stirred under reflux for 1 hour then cooled to room temperature and filtered. Washed thoroughly with acetic acid, methanol and diethyl ether to give the product as an orange solid (5.76 g, 72%). FTIR ν_{max}/cm^{-1}: 3062 (N-H), 1734 (C=O, asym. str), 1674 (C=O, sym. str).

N,N'-bis(8-bromooctyl)-1,4,5,8-naphthalenetetracarboxylic diimide (3)

The synthesis is based on previous work by Nakano *et al.*[7] **2** (1.70 g, 6.38 mmol) and 1-bromooctanol (3.28 mL, 19.1 mmol) were stirred in anhydrous THF (30 mL) and cooled to 0 °C. A solution of diethyl azodicarboxylate (3.77 mL, 19.1 mmol) and triphenylphosphine (5.02 g, 19.1 mmol) in anhydrous THF (20 mL) was then added to this dropwise under a nitrogen atmosphere and the reaction was stirred at room temperature overnight. Solvent was evaporated and the crude oil was run through a short silica plug with DCM as eluent. Further purification by column chromatography (3:7 hexane:DCM) and recrystallisation from ethyl acetate/hexane gave the pure product as yellow crystals (0.801 g, 21%). ^{1}H NMR (700 MHz, $CDCl_3$) δ 8.75 (4H, s, Ar*H*), 4.19 (4H, t, *J* = 7.7 Hz, NC*H*$_2$), 3.40 (4H, t, *J* = 6.9 Hz, C*H*$_2$Br), 1.85 (4H, quin, *J* = 7.2 Hz, NCH$_2$C*H*$_2$), 1.74 (4H, quin, *J* = 7.6 Hz, C*H*$_2$CH$_2$Br), 1.32-1.45 (16H, m, (C*H*$_2$)$_4$); ^{13}C NMR (176 MHz, $CDCl_3$) δ 163.0 (N*C*O), 131.1 (Ar*C*), 126.8 (Ar*C*), 126.8 (Ar*C*), 41.0 (*C*H$_2$N(CH$_3$)$_3$), 34.1 *C*H$_3$Br), 32.1 (*C*H$_2$), 29.2 (*C*H$_2$), 28.7 (*C*H$_2$), 28.2 (*C*H$_2$), 28.1 (*C*H$_2$), 27.0 (*C*H$_2$); HRMS (ESI) *m/z*: 647.1105; calculated for $[C_{30}H_{36}Br_2N_2O_4+H]^+$ = 647.1120

N,N'-bis(8-(trimethylammoniumbromide)octylene)-1,4,5,8-naphthalenetetracarboxylic diimide (NDI-NMe$_3$Br)

Following on from work by Xu *et al.* [8], **3** (383 mg, 0.590 mmol), trimethylamine hydrochloride (226 mg, 2.36 mmol) and sodium bicarbonate (248 mg, 2.95 mmol) were dissolved in anhydrous acetonitrile (20 mL) and heated to 80 °C for 20 h. The reaction mixture was cooled to room temperature and some orange precipitate formed which was redissolved by adding 10 mL methanol. The mixture was then filtered, and the filtrate was concentrated by rotary evaporation. The crude solid was then recrystallised in methanol/ethyl acetate which gave the pure product as orange crystals (229 mg, 51%). ^{1}H NMR (400 MHz, D_2O) δ 8.26 (4H, s, Ar*H*), 3.93 (4H, t, *J* = 7.8 Hz, NC*H*$_2$), 3.37 (4H, m, C*H*$_2$N(CH$_3$)$_3$Br), 3.14 (18H, s, N(C*H*$_3$)$_3$Br), 1.85 (4H, m, C*H*$_2$), 1.67 (4H, m, C*H*$_2$), 1.45 (16H, m, (C*H*$_2$)$_4$); ^{13}C NMR (100 MHz, D_2O) δ 163.7 (N*C*O), 131.3 (Ar*C*), 125.9 (Ar*C*), 125.6 (Ar*C*), 67.3 (*C*H$_2$N(CH$_3$)$_3$), 53.4 (N(*C*H$_3$)$_3$), 41.5 (N*C*H$_2$), 28.7 (*C*H$_2$), 27.6 (*C*H$_2$), 26.7 (*C*H$_2$), 26.0 (*C*H$_2$), 22.8 (*C*H$_2$); HRMS (ESI) *m/z*:303.2067; calculated for $[C_{36}H_{52}N_4O_4+H]^{2+}$ = 303.2066

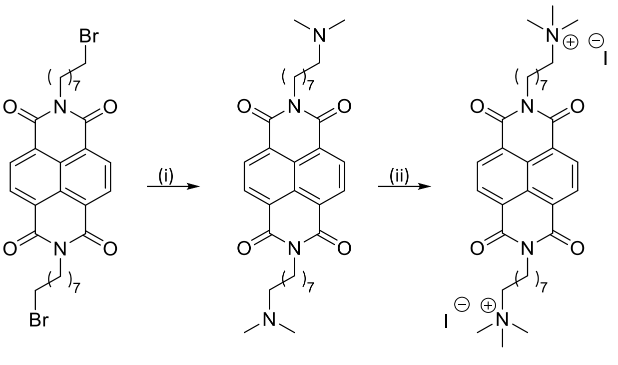

3 **4** **5**

Scheme S2. *Synthesis of NDI-NMe$_3$I. Reagents and conditions: (i) NHMe$_2$, THF, reflux 16 h. (ii) MeI, CHCl$_3$, reflux 2 h.*

N,N'-bis(8-(trimethylammoniumiodide)octylene)-1,4,5,8-naphthalenetetracarboxylic diimide (5)

3 (0.500 g, 0.770 mmol) and dimethylamine (2.00 M in THF, 38.6 mL, 77.1 mmol) were dissolved in anhydrous THF (25 mL) and stirred under reflux overnight in a nitrogen atmosphere. Reaction mixture was cooled to room temperature and excess dimethylamine was removed by bubbling with a stream of nitrogen for 2 hours. Solvent THF was removed in vacuo to give **4** as a crude oil. The resultant oil was then dissolved in chloroform (27 mL) and iodomethane (0.290 mL, 3.86 mmol) was added before being refluxed for 2 hours. The reaction mixture was cooled to room temperature and a brown precipitate was filtered and washed with chloroform, hexane, ethanol, and diethyl ether before being recrystallised from acetone/water to give the product as an orange solid (0.296 g, 44%). ^{1}H NMR (700 MHz, DMSO) δ 8.64 (4H, s, Ar*H*), 4.04 (4H, t, *J* = 7.7 Hz, NC*H*$_2$), 3.27 (4H, m, C*H*$_2$N(CH$_3$)$_3$I), 3.04 (18H, s, N(C*H*$_3$)$_3$I), 1.63-1.68 (8H, m, NCH$_2$(C*H*$_2$)$_2$), 1.31-1.39 (12H, m, (C*H*$_2$)$_3$), 1.28 (4H, m, C*H*$_2$); ^{13}C NMR (176 MHz, DMSO) δ 162.6 (N*C*O), 130.5 (Ar*C*), 126.3 (Ar*C*), 126.2 (Ar*C*), 65.3 (*C*H$_2$N(CH$_3$)$_3$), 52.2 (N(*C*H$_3$)$_3$), 40.1 (N*C*H$_2$), 28.5 (*C*H$_2$), 28.4 (*C*H$_2$), 27.4 (*C*H$_2$), 26.5 (*C*H$_2$), 25.7 (*C*H$_2$), 22.0 (*C*H$_2$); HRMS (ESI) *m/z*: 303.2068; calculated for $[C_{36}H_{52}N_4O_4+H]^{2+}$ = 303.2067

IR spectrum of 1,4,5,8-Naphthanlenetetracarboxylic diimide (2)

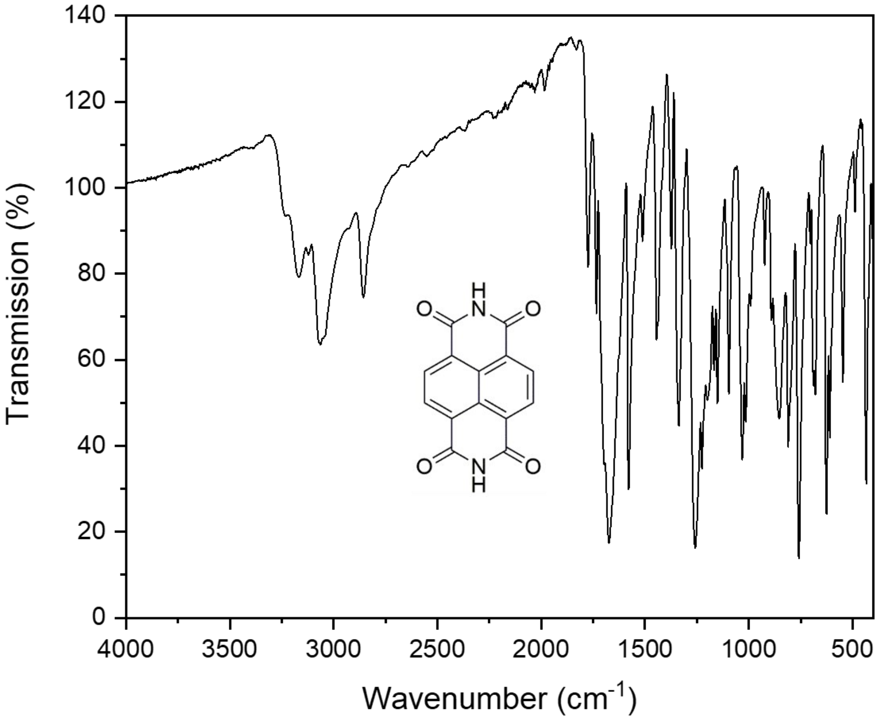

^{1}H and ^{13}C-NMR spectrum of *N,N'*-bis(8-bromooctyl)-1,4,5,8-naphthalenetetracarboxylic diimide (3)

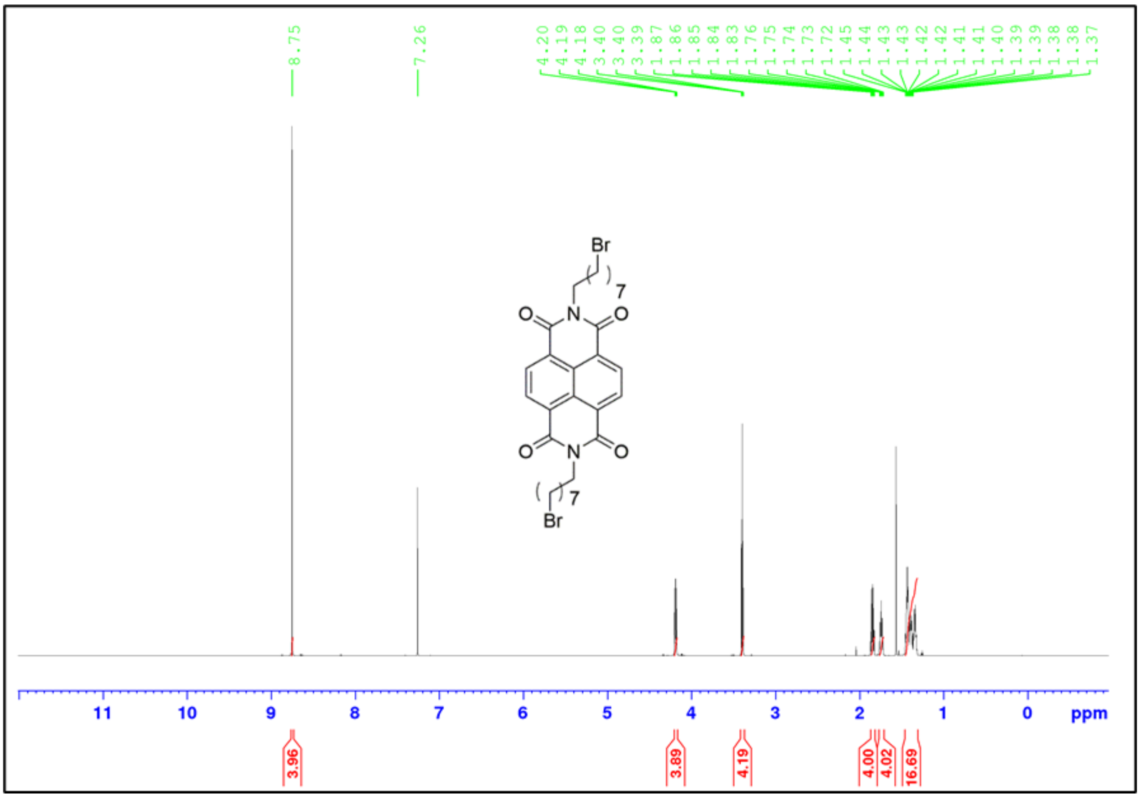

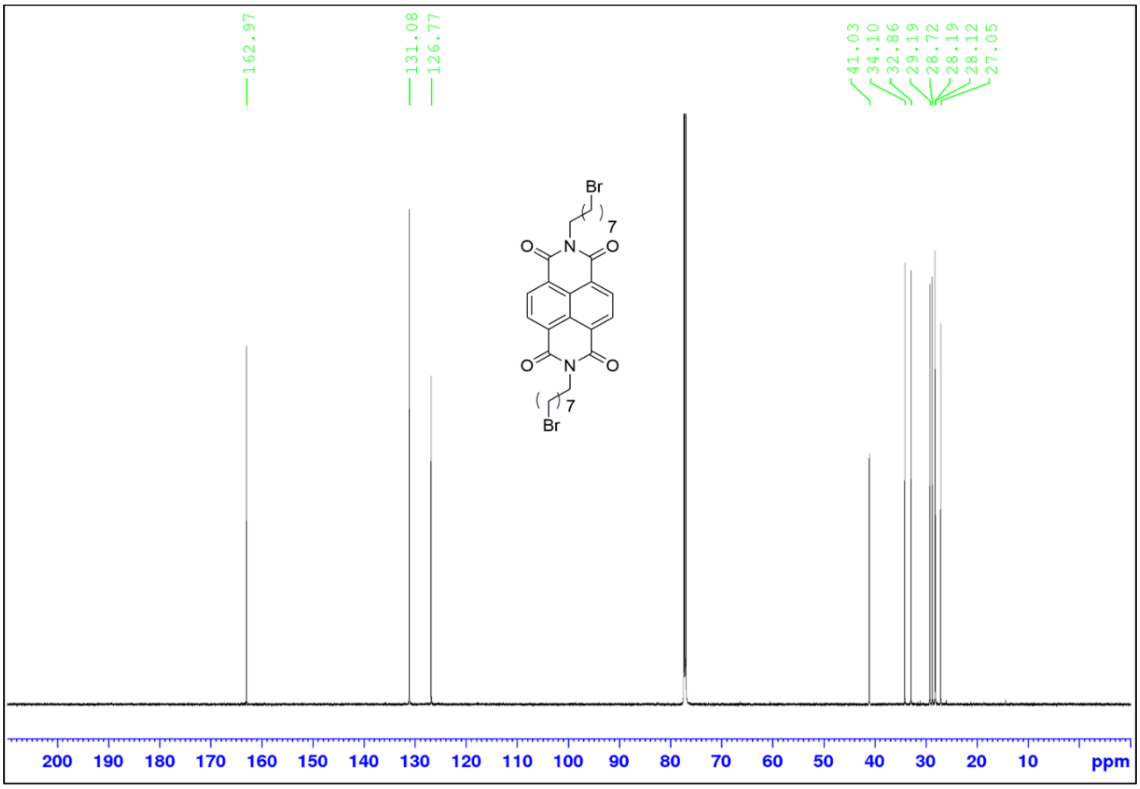

^{1}H and ^{13}C-NMR spectrum of *N,N'*-bis(8-(trimethylammoniumbromide)octylene)-1,4,5,8-naphthalenetetracarboxylic diimide (NDI-NMe$_3$Br)

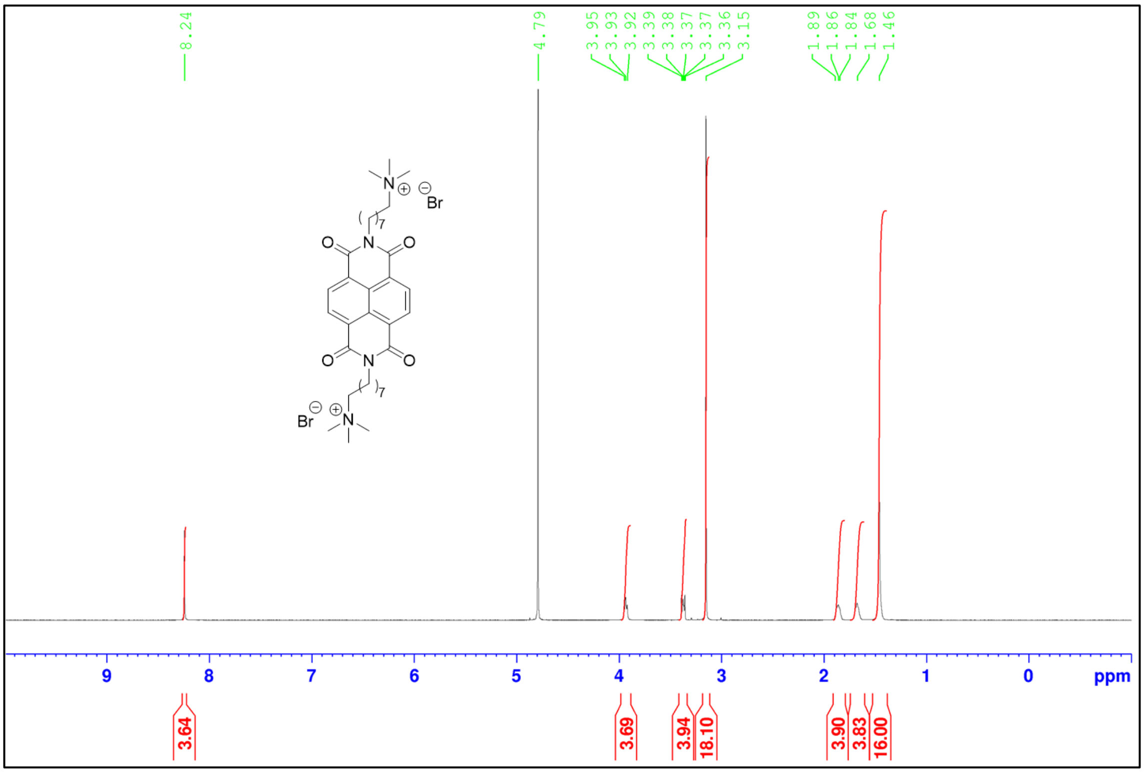

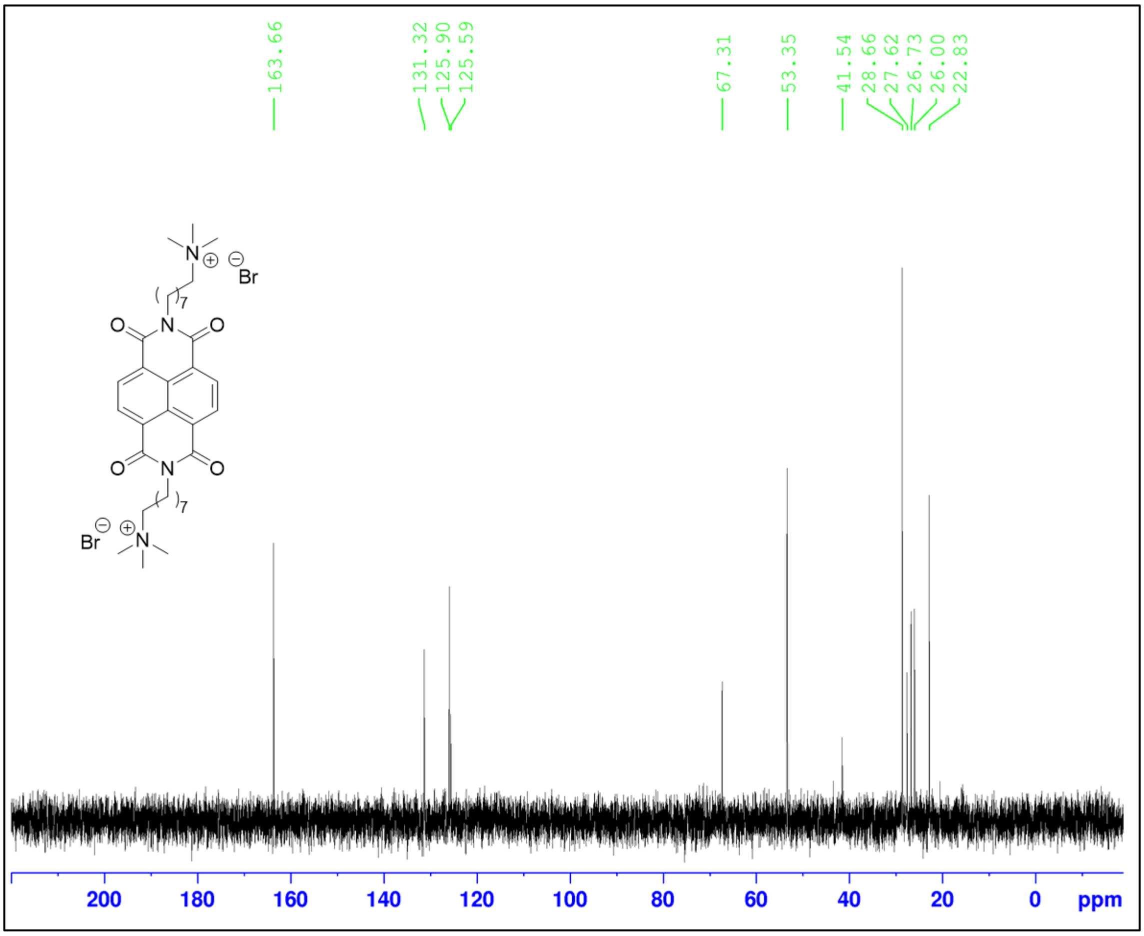

Table S1. X-ray fluorescence (XRF) analysis of NDI-NMe$_3$Br showing concentration of elements present in powder sample.

Compound	Concentration
Br	94.364 wt%
Cl	3.422 wt%
P	1.455 wt%
Ca	0.480 wt%
Sn	0.133 wt%
Si	791.3 ppm
Te	302.6 ppm
Fe	173.2 ppm
Mn	109.7 ppm
Cr	67.1 ppm
Eu	23.2 ppm

^{1}H and ^{13}C-NMR spectrum of *N,N'*-bis(8-(trimethylammoniumiodide)octylene)-1,4,5,8-naphthalenetetracarboxylic diimide (5)

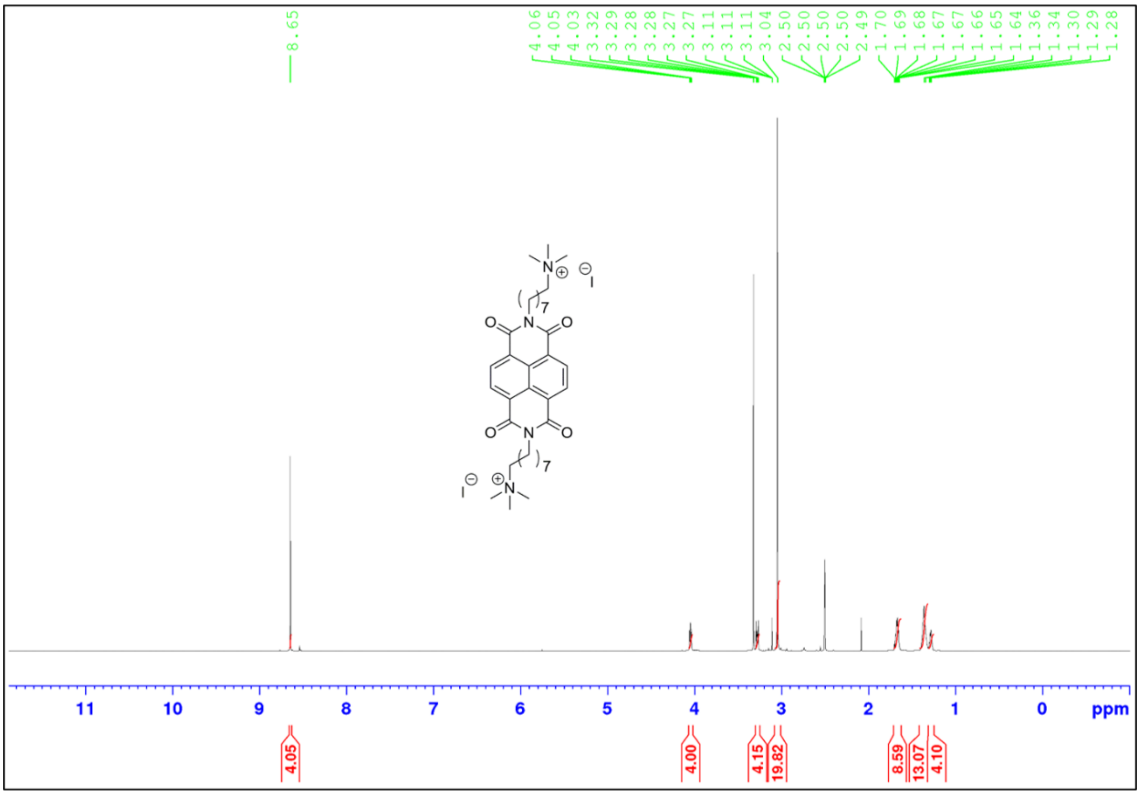

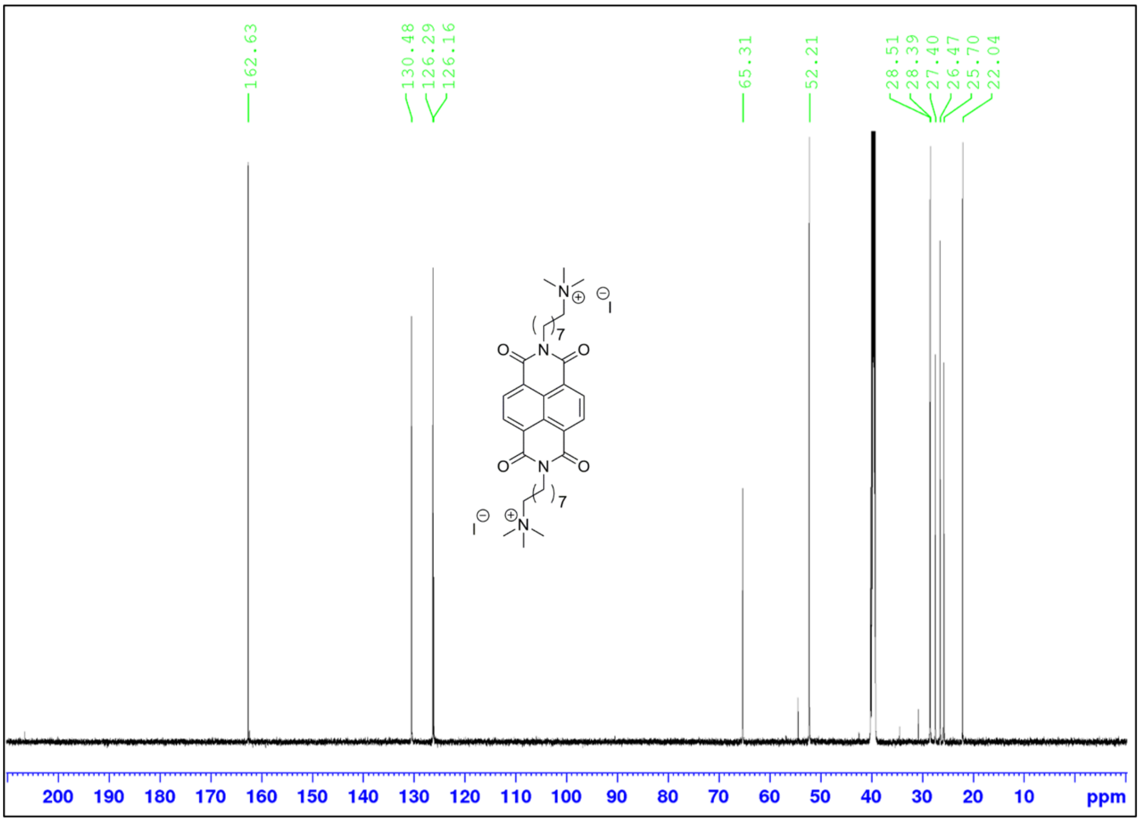

Structural Characterisation of NDI-OH and Doped Films

Procedure for ion-exchange to form *N,N'*-Bis(8-(trimethylammoniumhydroxide)octylene)-1,4,5,8-naphthalenetetrabarboxylic diimide (NDI-OH):

NDI-NMe₃Br (50 mg) was dissolved in 5 mL deionised water (or deuterium oxide for NMR samples). A column of ion-exchange resin (DOWEX 550A, Sigma) was made up and washed with deionised water. The **NDI-NMe₃Br** solution was loaded on the column and slowly eluted using 5 mL deionised water (or deuterium oxide) to wash through. This gave an approximately 5 mg mL^{-1} colourless solution of **NDI-OH**. See Figure S1 to Figure S8 for structural characterisation.

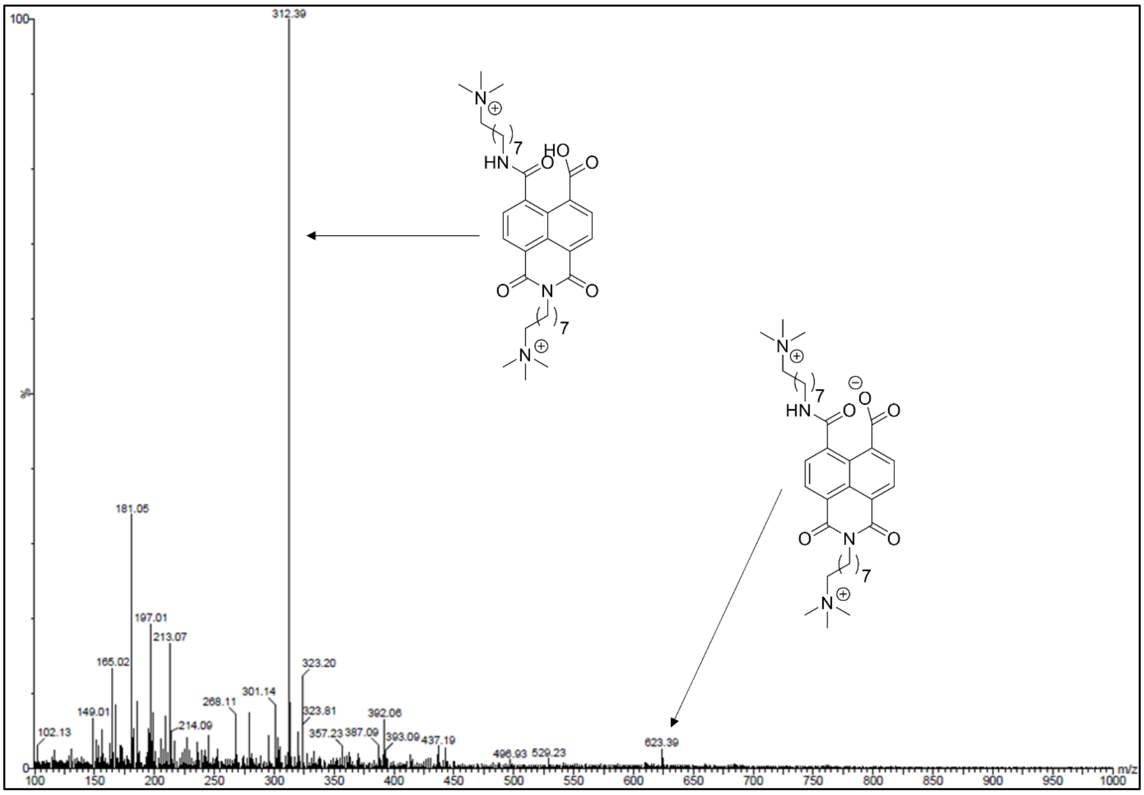

Figure S1. *Mass spectrum of a solution of NDI-OH immediately after ion-exchange column.*

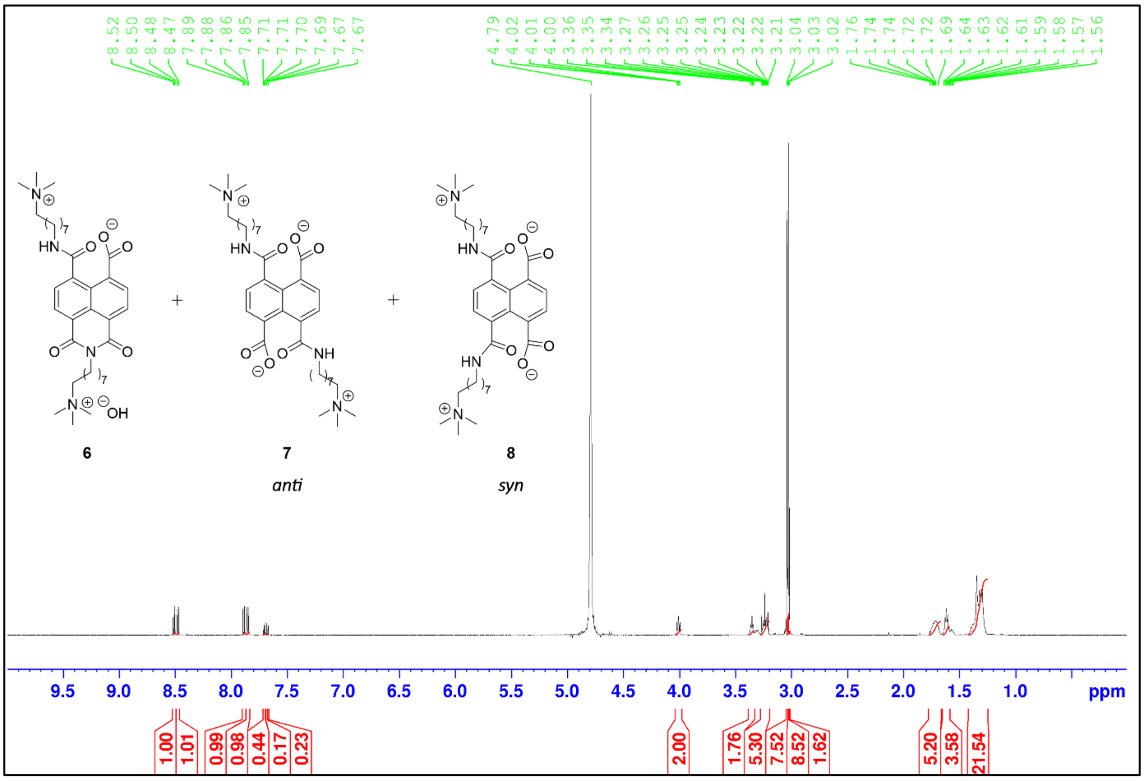

Figure S2. *Full ^{1}H NMR spectrum of NDI-OH. Products of hydrolysis discussed in the main text are shown.*

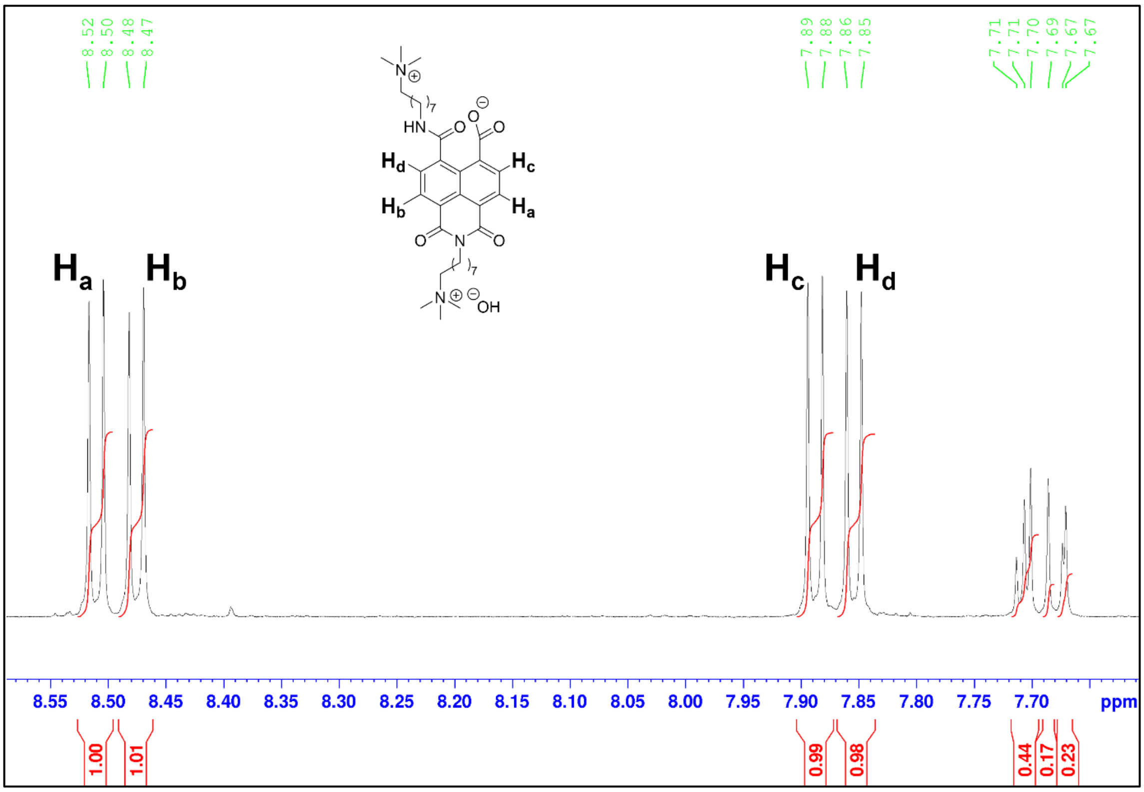

Figure S3. *^{1}H NMR spectrum of NDI-OH between 8.55 ppm and 7.65 ppm.*

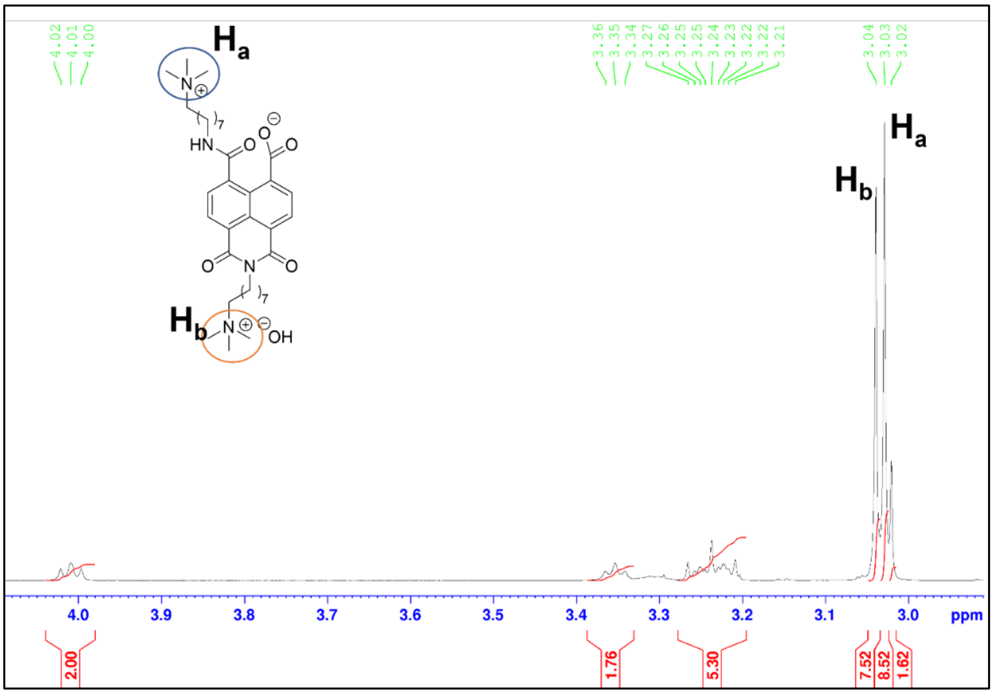

Figure S4. *^{1}H NMR spectrum of NDI-OH between 4.10 ppm and 2.90 ppm.*

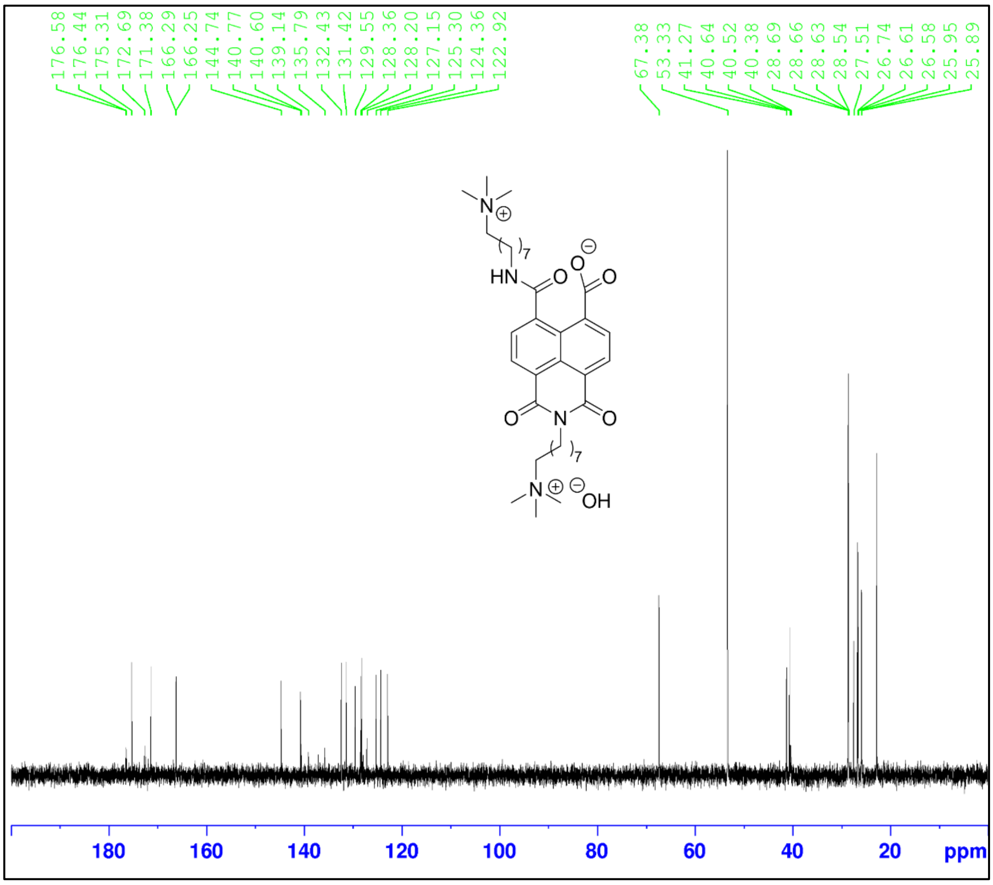

Figure S5*. Full ^{13}C NMR spectrum of NDI-OH.*

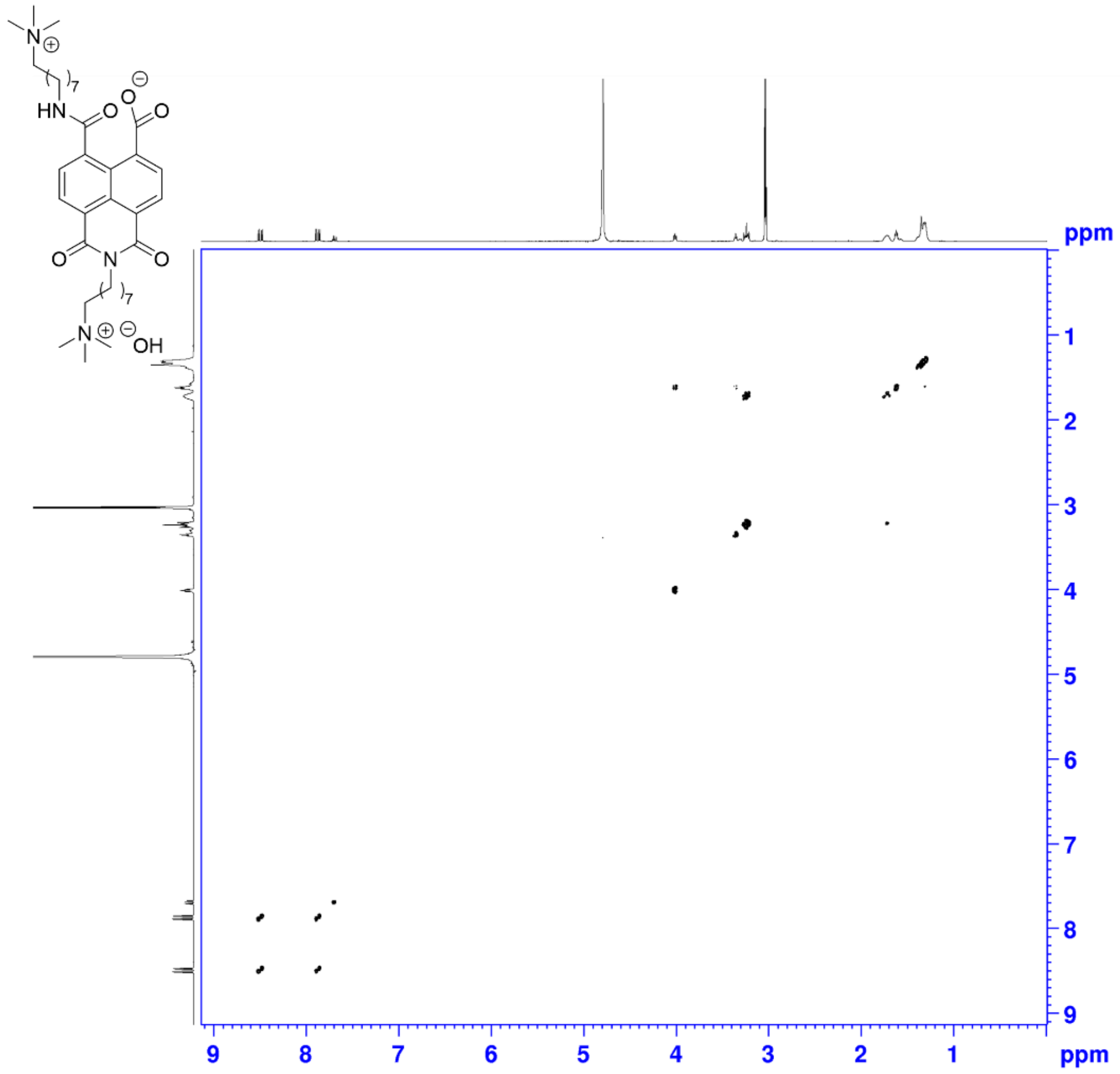

Figure S6. *2D ^1H-^1H correlation spectroscopy (COSY) of NDI-OH in D2O.*

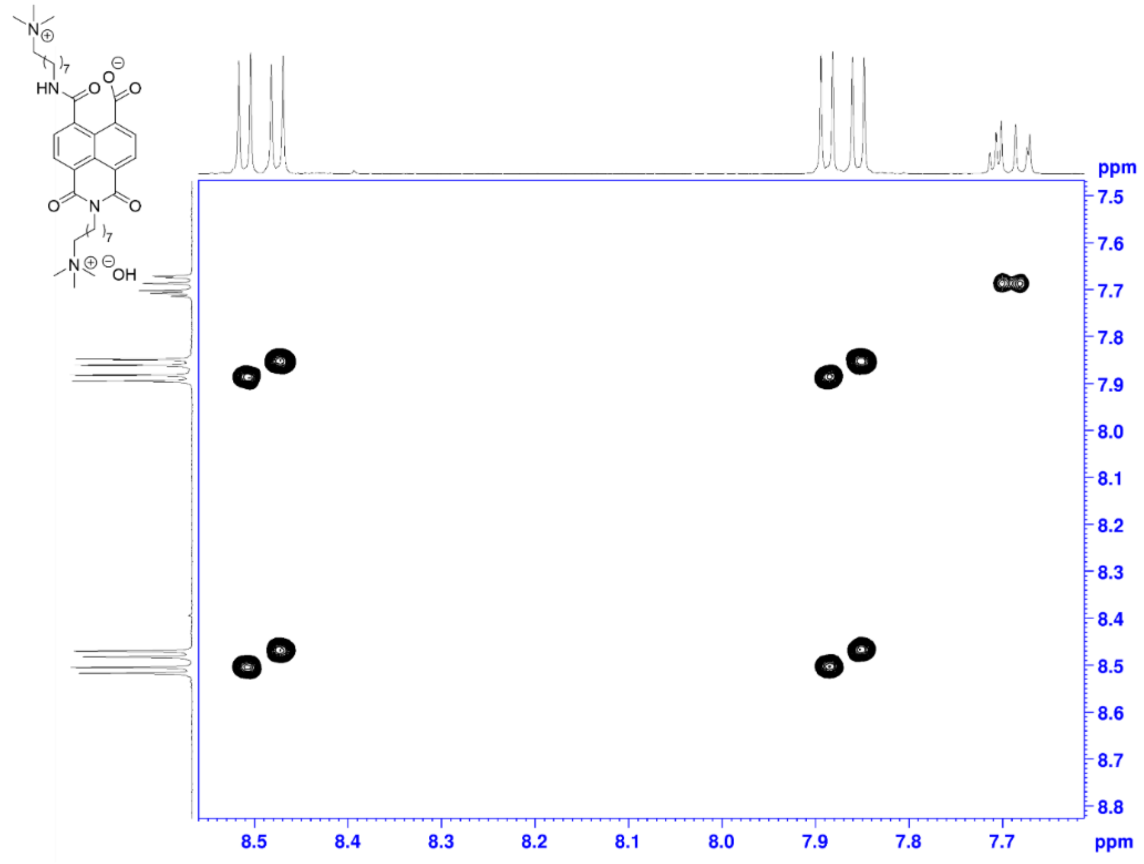

Figure S7. *2D* ^{1}H-^{1}H *correlation spectroscopy (COSY) of the aromatic region of NDI-OH in D2O.*

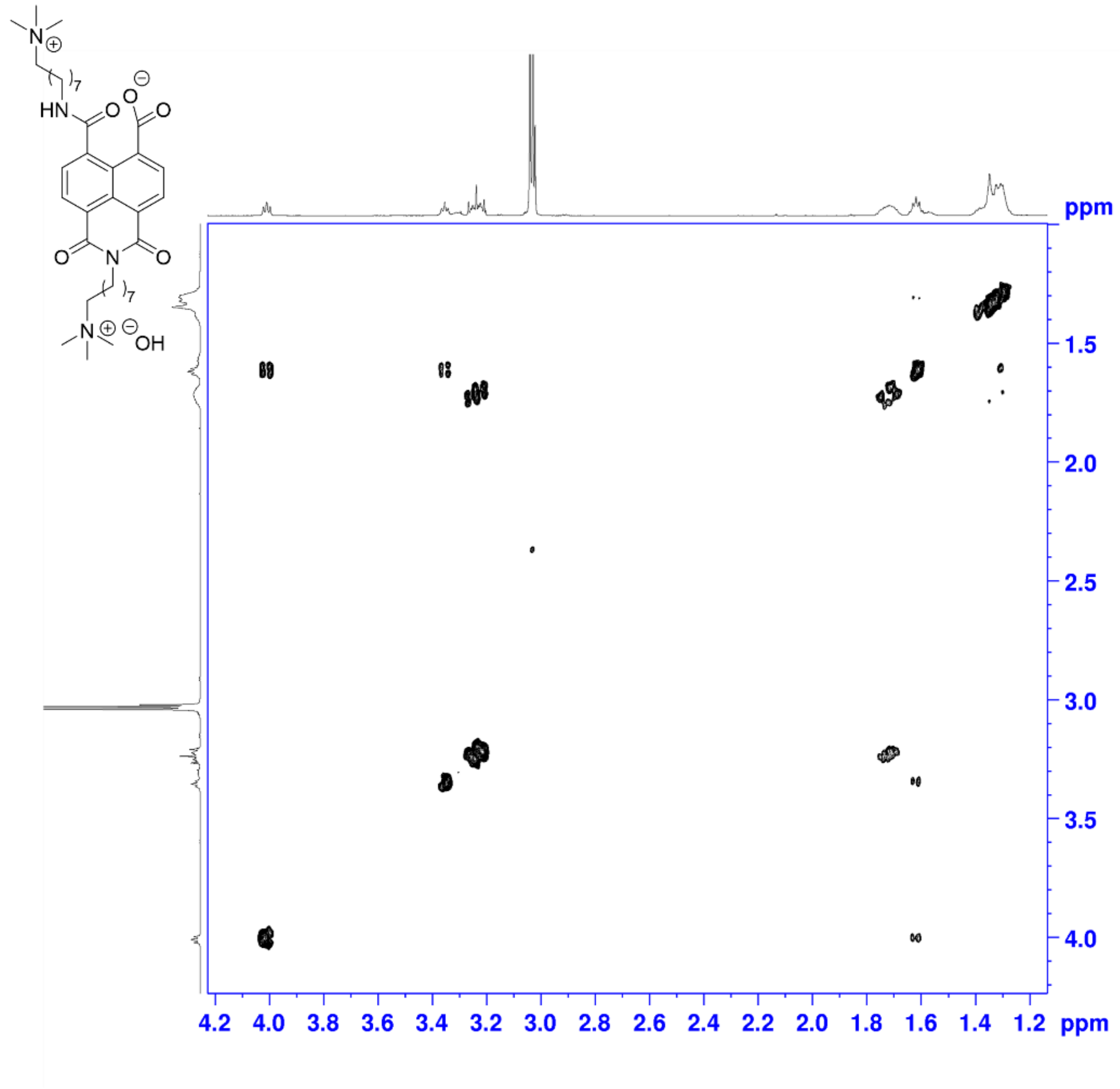

Figure S8. *2D ^{1}H-^{1}H correlation spectroscopy (COSY) of NDI-OH in D2O between 4.2 and 1.2 ppm.*

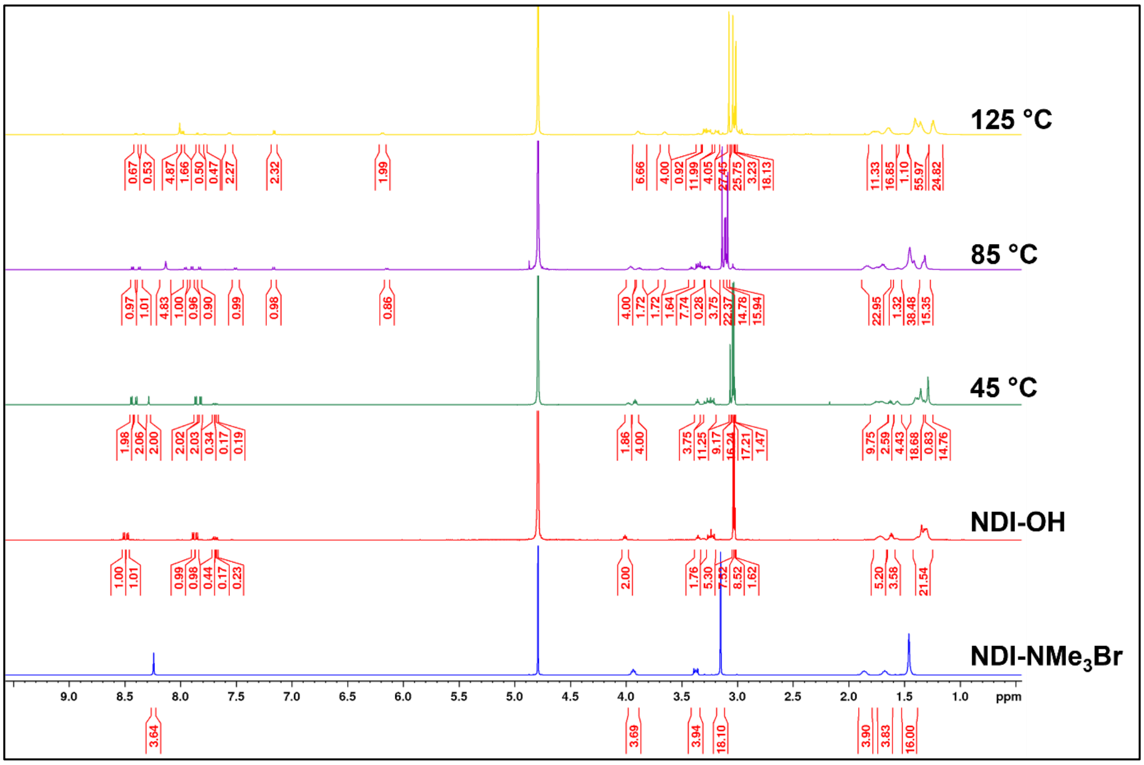

Figure S9. *Comparison of ^{1}H NMR spectra for NDI-NMe$_3$Br, NDI-OH solution and films drop-cast at 45 °C, 85 °C and 125 °C.*

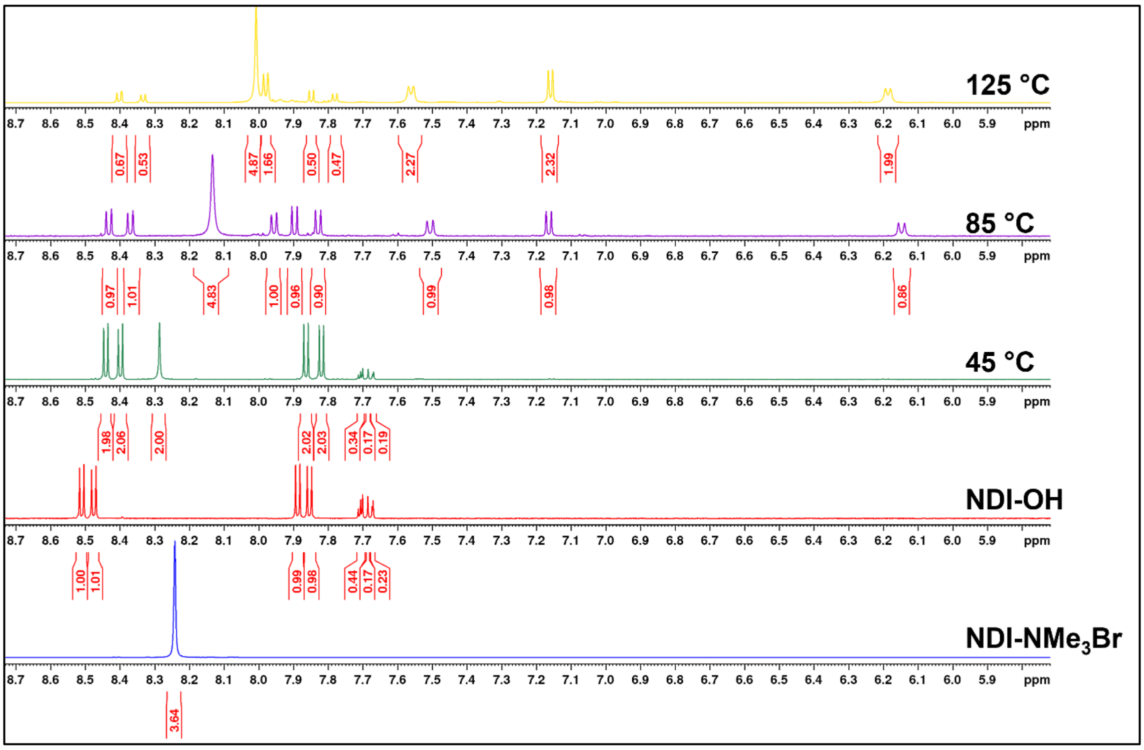

Figure S10. *Comparison of the aromatic regions of ^{1}H NMR spectra for NDI-NMe$_3$Br, NDI-OH solution and films drop-cast at 45 °C, 85 °C and 125 °C.*

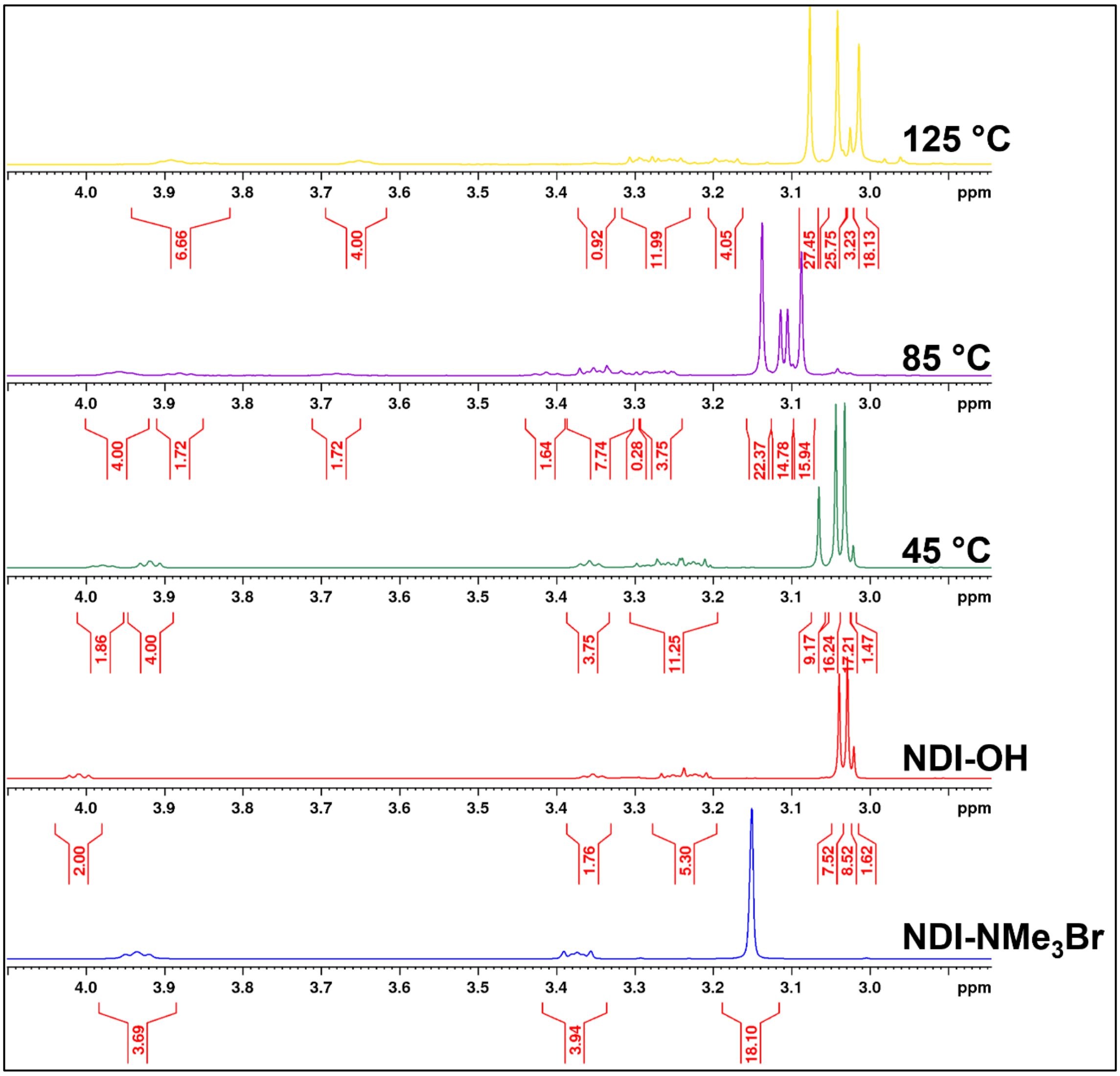

Figure S11. *Comparison of ^{1}H NMR spectra for NDI-NMe$_3$Br, NDI-OH solution and films drop-cast at 45 °C, 85 °C and 125 °C between 4.1 and 2.9 ppm.*

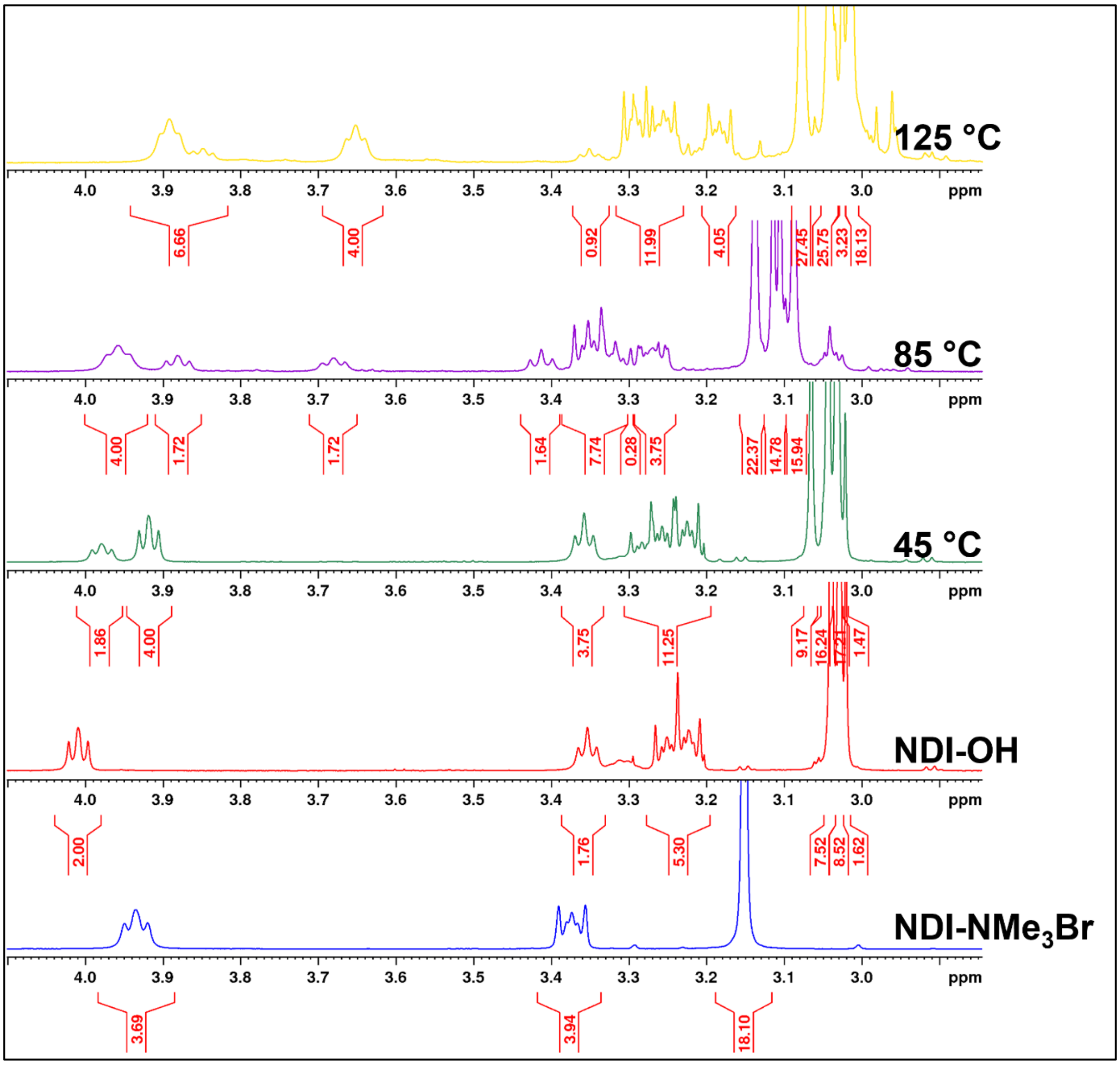

Figure S12. *Comparison of ^{1}H NMR spectra for NDI-NMe$_3$Br, NDI-OH solution and films drop-cast at 45 °C, 85 °C and 125 °C between 4.1 and 2.9 ppm.*

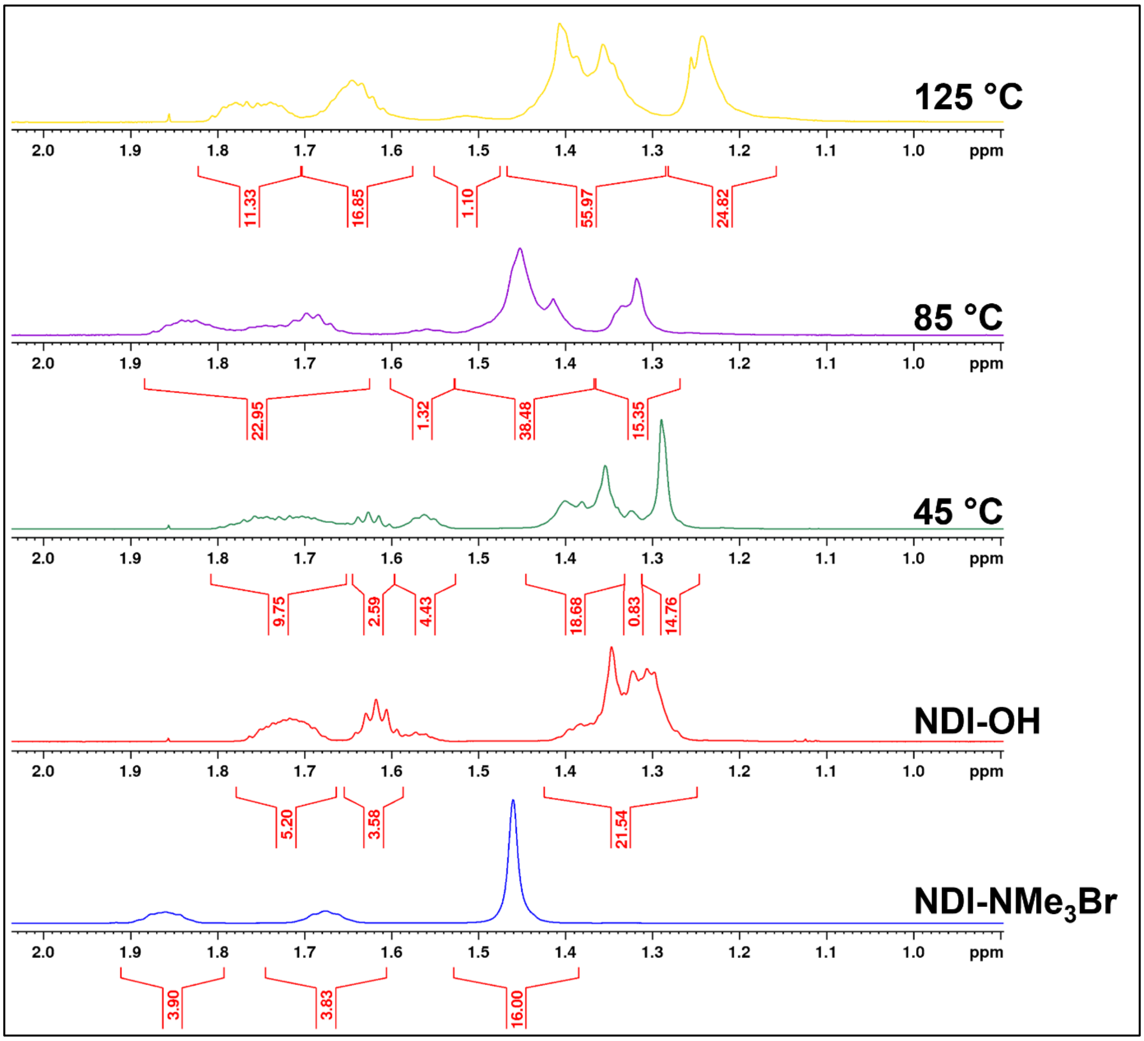

Figure S13. *Comparison of ^{1}H NMR spectra for NDI-NMe$_3$Br, NDI-OH solution and films drop-cast at 45 °C, 85 °C and 125 °C between 2.0 and 0.9 ppm.*

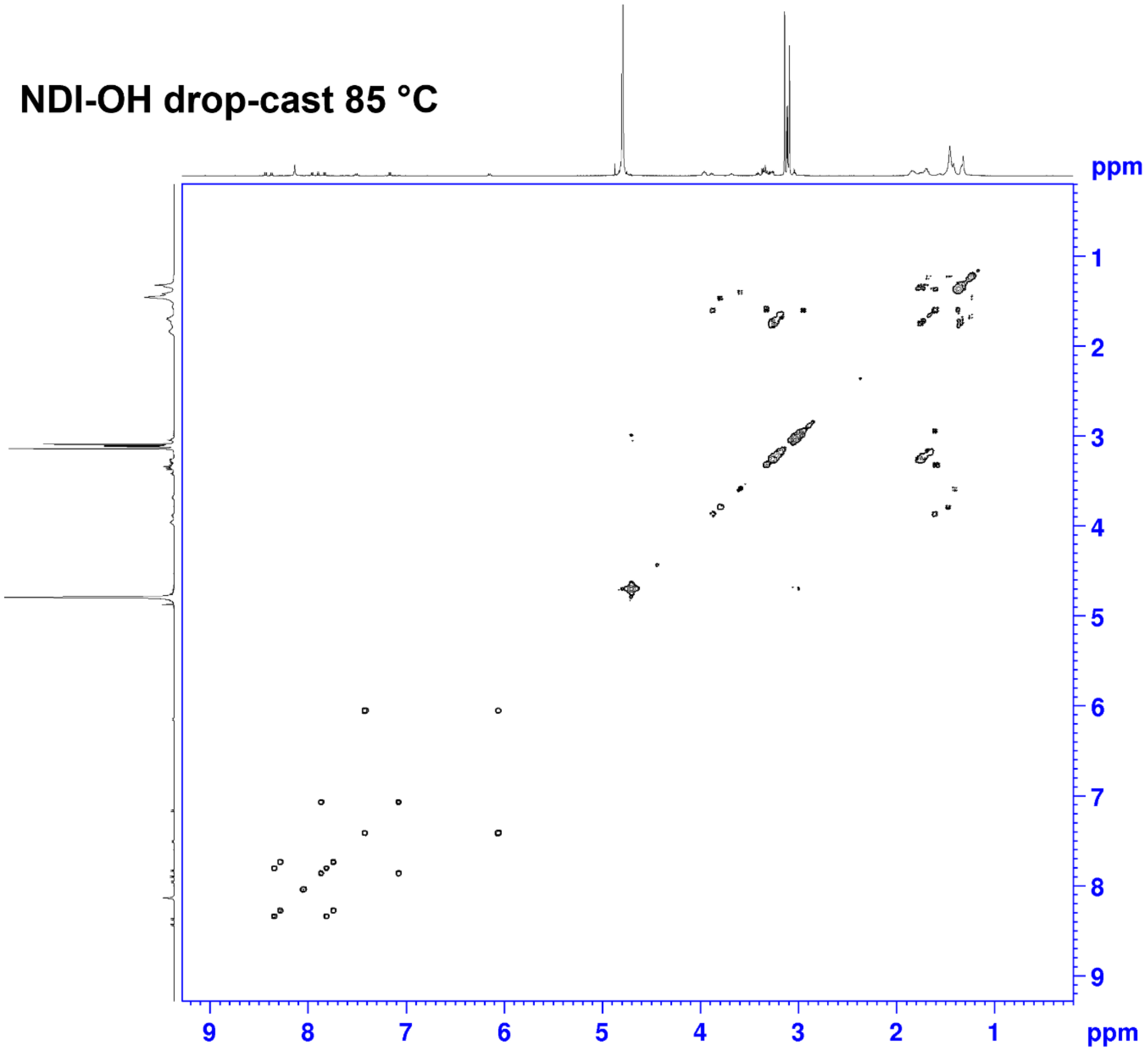

Figure S14. *2D ^{1}H-^{1}H correlation spectroscopy (COSY) of NDI-OH film drop-cast at 85 °C redissolved in D_2O.*

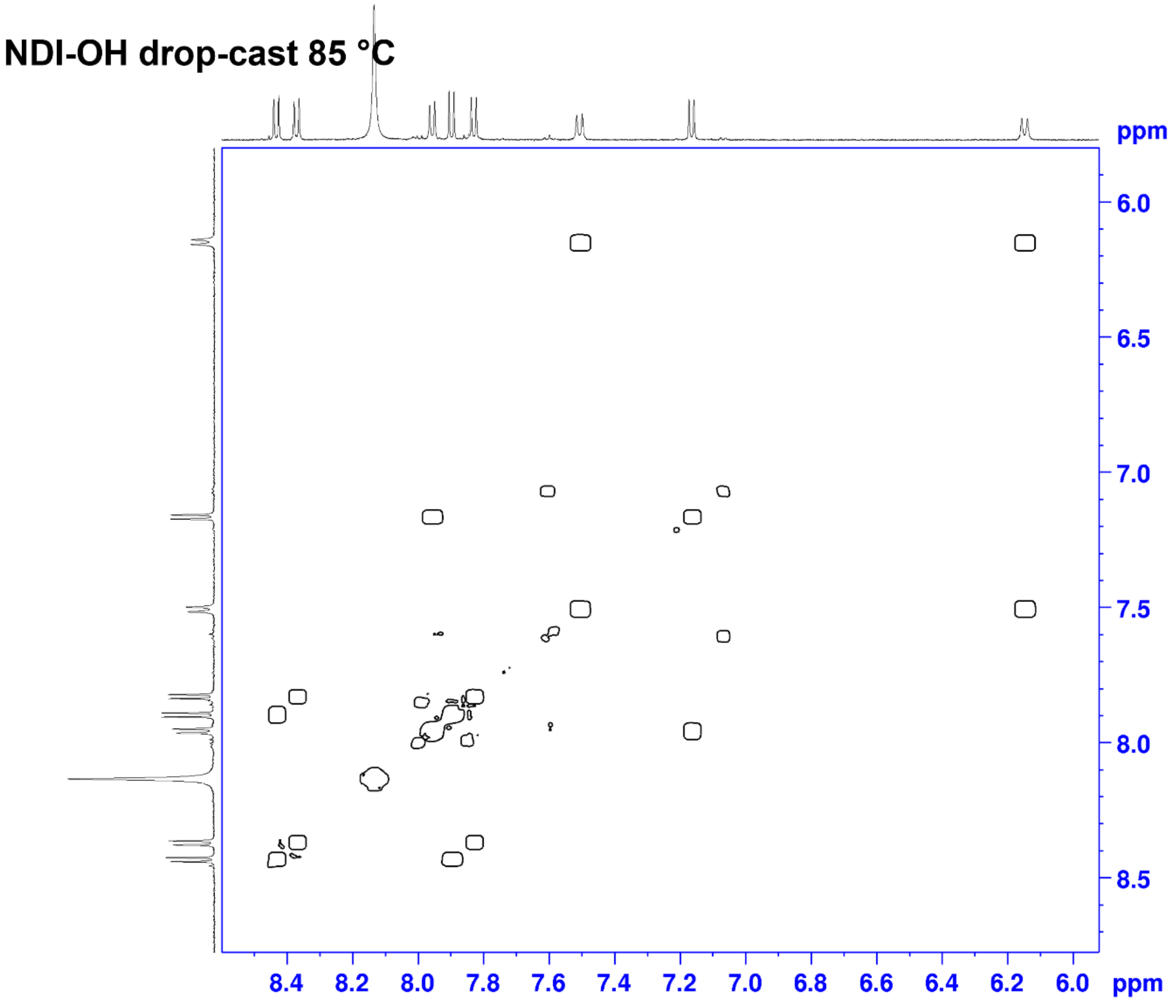

Figure S15. *2D ^{1}H-^{1}H correlation spectroscopy (COSY) of NDI-OH film drop-cast at 85 °C redissolved in D_2O between 6.5 and 8.5 ppm.*

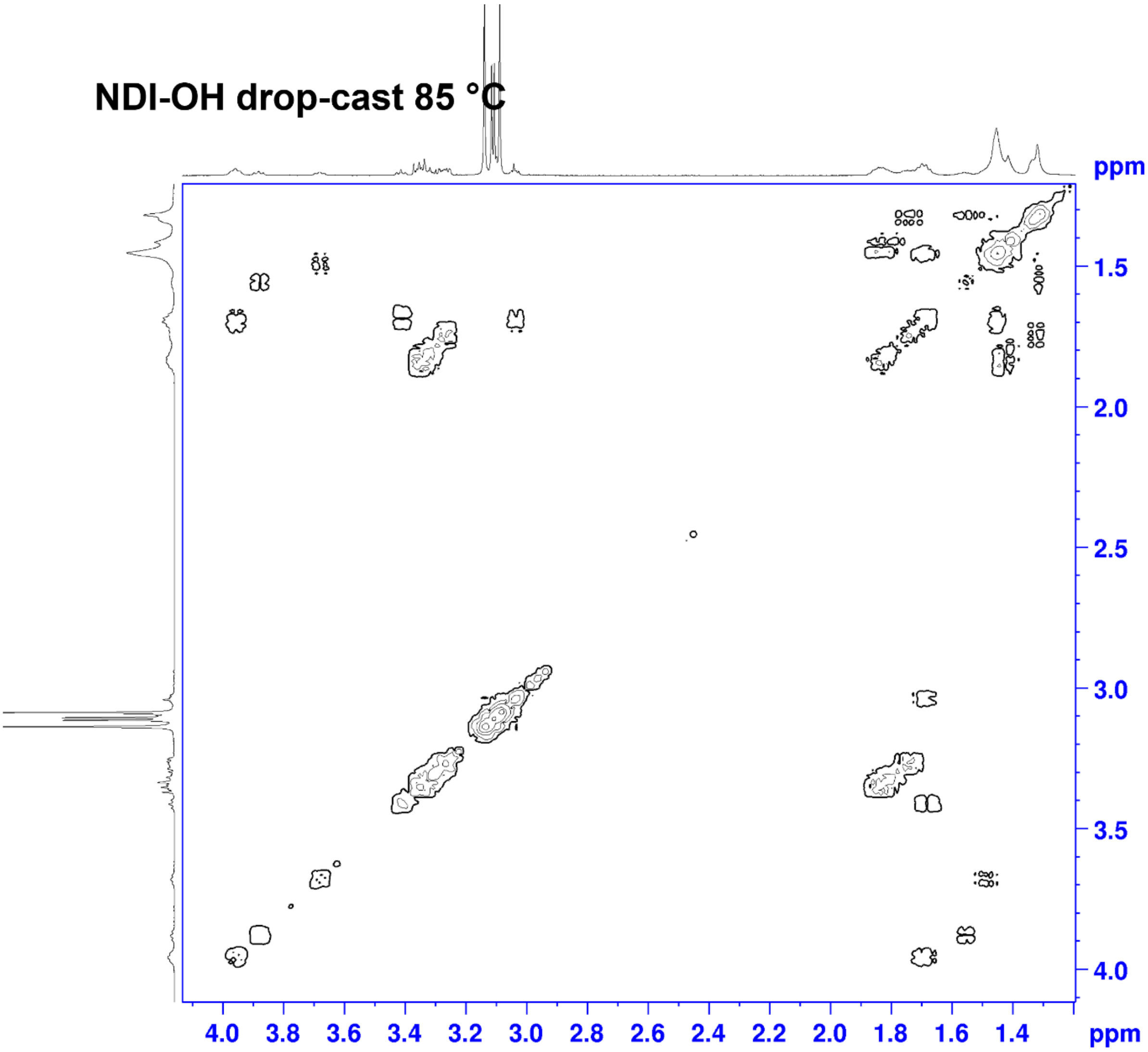

Figure S16. *2D ^{1}H-^{1}H correlation spectroscopy (COSY) of NDI-OH film drop-cast at 85 °C redissolved in D_2O between 1.3 and 4.0 ppm.*

Cyclic Voltammetry

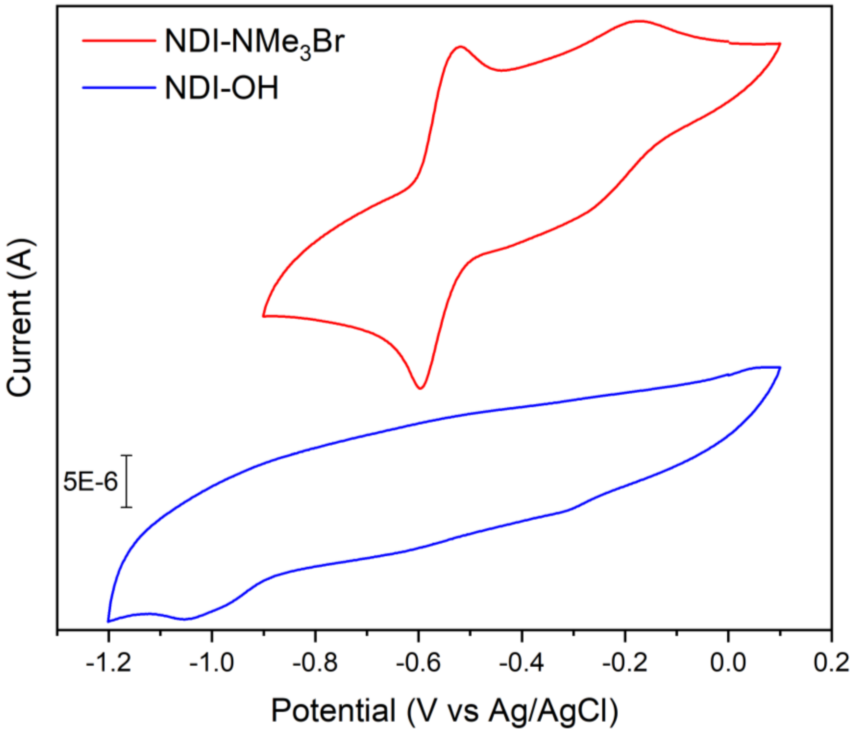

Figure S17. *Cyclic voltammograms of NDI-NMe$_3$Br and NDI-OH run in aqueous solutions of 3 M KCl as electrolyte. Glassy carbon was used as working electrode, platinum wire as counter electrode and silver/silver chloride (Ag/Ag$^+$) reference electrode. Values are reported from the 4th cycle and measured at 100 mV.s^{-1}.*

Electron Paramagnetic Resonance

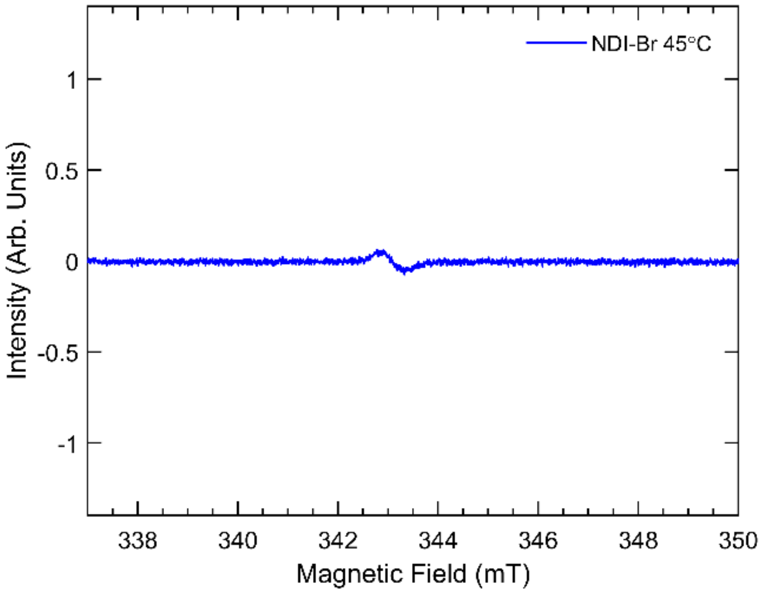

Figure S18. *EPR spectrum of NDI-Br thin-film drop cast at 45 °C.*

Grazing Incidence Wide Angle X-ray Scattering

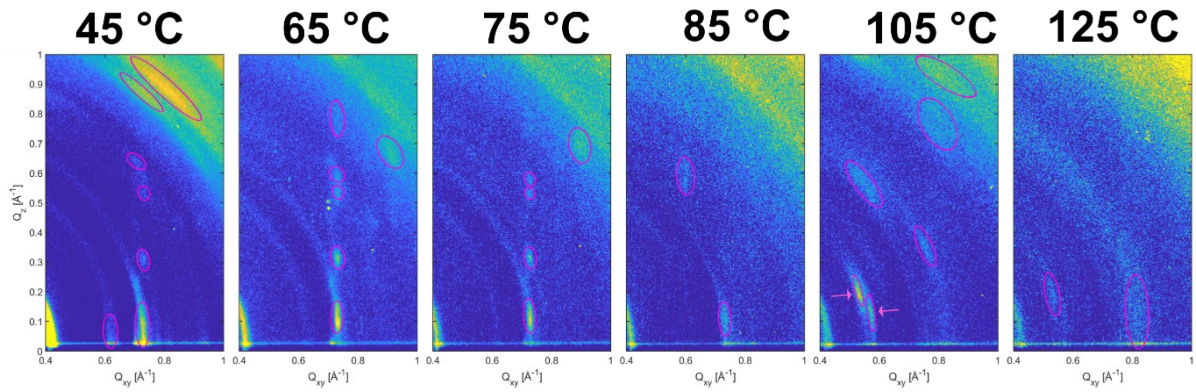

Figure S19. *2D GIWAXS measurements of NDI-OH films drop-cast at temperatures between 45 °C and 125 °C, focused on the region from Q_{xy} = 0.4 Å^{-1} to Q_{xy} = 1 Å^{-1}. Ellipses are drawn to guide the eye.*

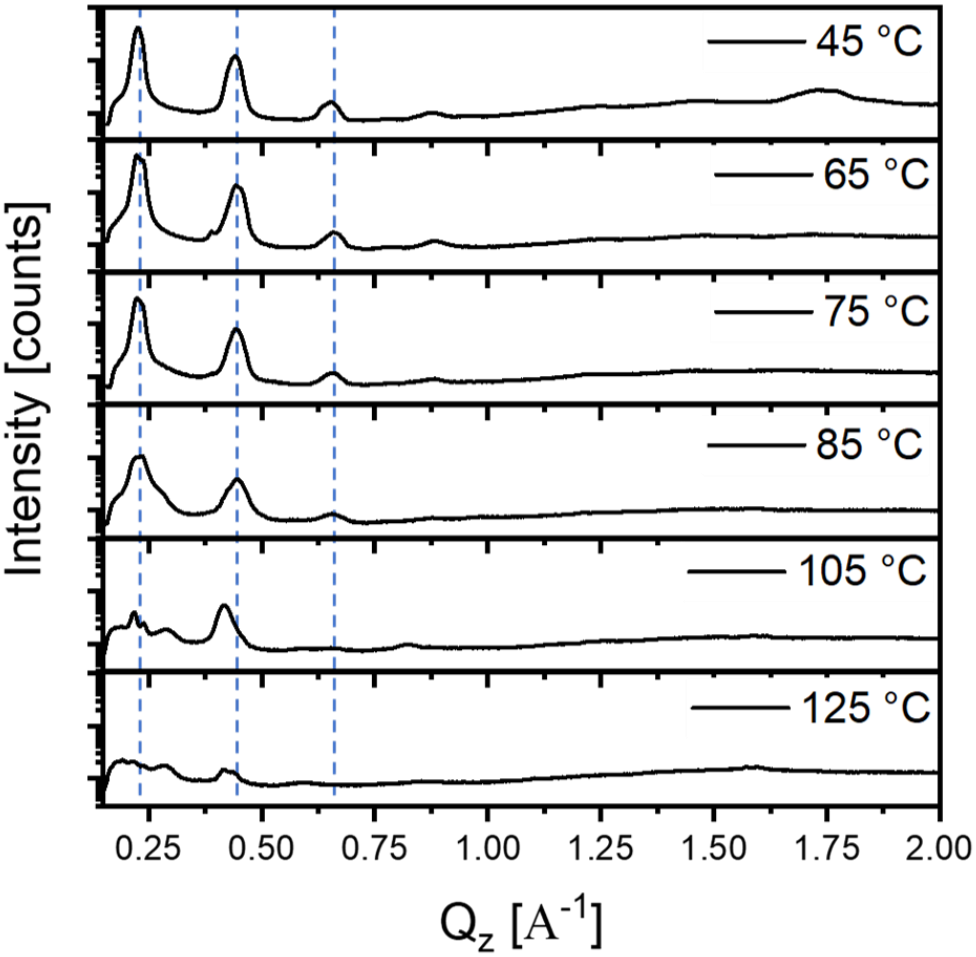

Figure S20. *1D scattering profile of NDI-OH thin films in the Q_z direction.*

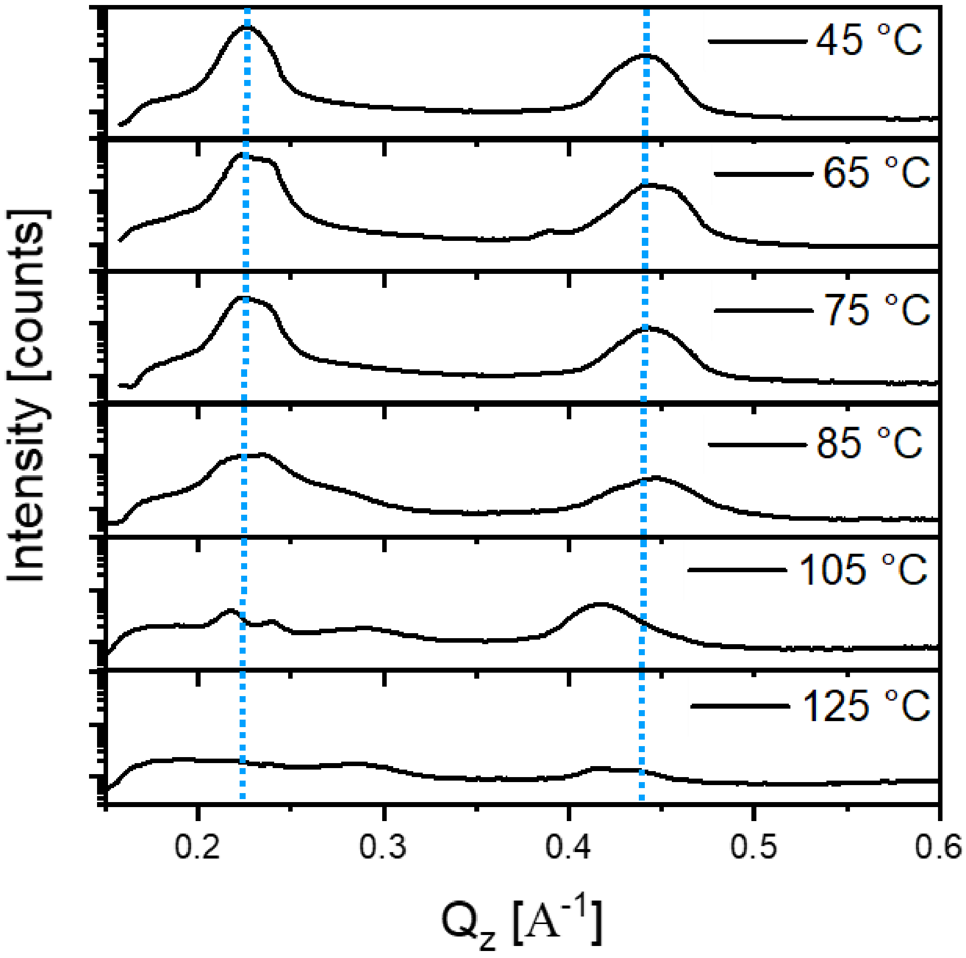

Figure S21. *1D scattering profile of NDI-OH thin films in the* Q_z *direction in region between* $Q_Z = 0.2$ Å^{-1} *and* $Q_Z = 0.6$ Å^{-1}.

Current - Voltage Characteristics of NDI-OH Doped Films

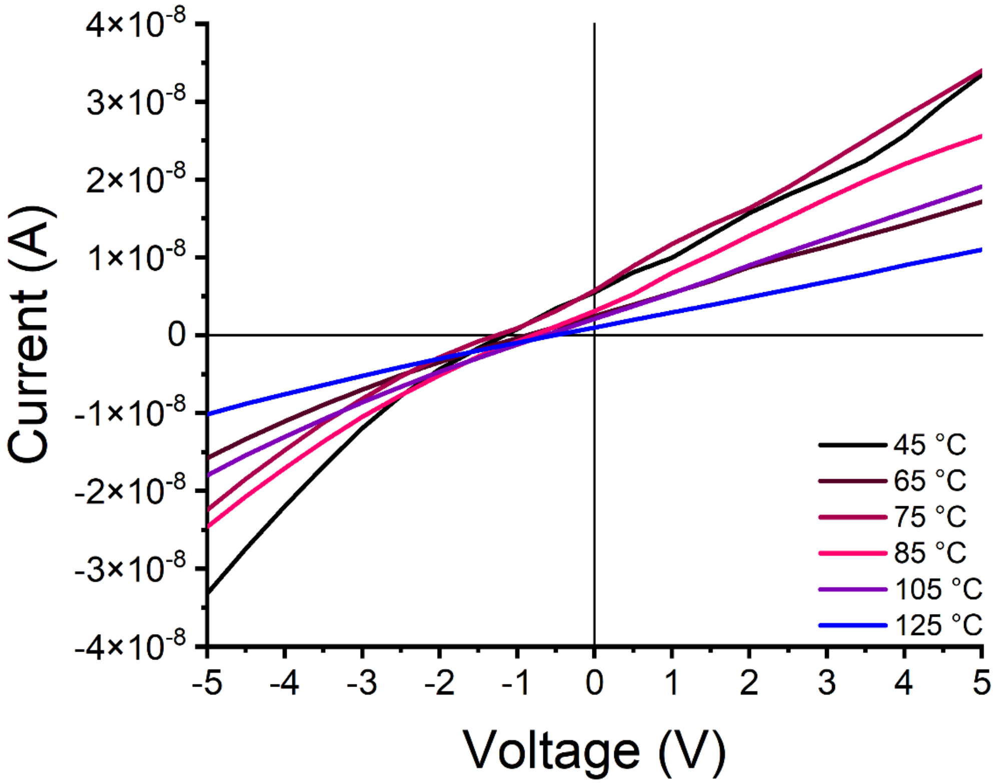

Figure S22. *I-V curves of NDI-OH films drop-cast at temperatures between 45 °C and 125 °C.*

Study of Quaternary Ammonium Breakdown and Possible Doping Species

The degradation of quaternary ammonium groups via a demethylation pathway (shown on the top left of Scheme S3) has been evidenced by the growth of XPS signals for tertiary amine nitrogens in drop-cast films of PDI-OH.[9] In addition, the bound dimethylamine product of demethylation has doped naphthalene diimides via a photo-induced pathway.[10] An alternative degradation is possible however and is shown in the bottom left of Scheme S3. This Hofmann elimination pathway has been shown to be favoured in heated alkyl quaternary ammonium hydroxides when *β*-hydrogens are available for abstraction.[11] It is possible therefore that in the formation of films of NDI-OH a Hofmann elimination occurs and the active doping species is instead trimethylamine (TMA). In order to test the efficacy of unbound tertiary amines acting as dopants to NDIs two different tertiary amines, TMA, and triethylamine (TEA), were used to dope a neutral water-soluble NDI derivative (NDI-TEG). Structures are shown on the right of Scheme S3.

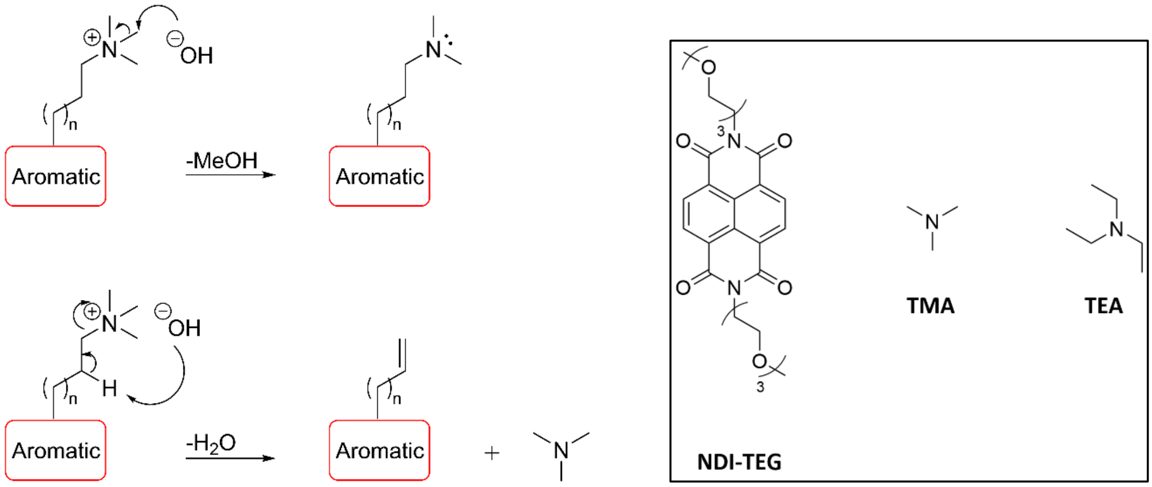

Scheme S3. *Previously proposed degradation of quaternary ammonium hydroxide moieties via an S_N2 substitution mechanism to form dimethylamine[9] (Top left). Possible degradation of the quaternary ammonium headgroup via an E2 Hofmann type elimination (bottom left). Structures of NDI-TEG, TMA and TEA used in this study.*

Initially 3 mg/mL aqueous solutions of NDI-TEG were made up and stirred at room temperature for 5 minutes with either 1 molar equivalent of TMA (from a 1 M solution in THF) or TEA. Solutions were then drop-cast on to glass slides at 45 °C, 65 °C, 75 °C, 85 °C, 105 °C and 125 °C. Figure S23 and Figure S24 show the UV-vis absorption spectra of the films compared to a drop-cast film of undoped NDI-TEG. For each film an absorption with maxima at approx. 350 nm can be seen in spectra for doped and undoped films drop-cast at each temperature. The absorptions attributed to doping at 450 nm in Figures 3b and 3c of the main text were not observed in doped NDI-TEG.

In order to better simulate the basic environment of NDI-OH solutions, NDI-TEG was also run through ion-exchange columns before doping with the two amines. Figure S25 and Figure S26 show the UV-vis absorption spectra of films made from drop-casting these solutions. No absorption was observed at about 450 nm for NDI-TEG doped with either TMA or TEA. The observation of no longer wavelength absorption at 450 nm for the less volatile TEA suggests that the reason for no doping is not the evaporation of low boiling TMA. In addition, the results go some way to supporting the demethylation pathway leading to the active doping species.

It is difficult to draw a full conclusion from these results alone, however. No positive identification of the products of Hofmann elimination or demethylation was provided by the NMR spectra of NDI-OH above and ionisation of the films for mass-spectrometry proved difficult. A combinatory technique, such as thermogravimetric analysis/mass-spectrometry used by Edson et al[11]., may help to positively identify some of the products of breakdown upon heating NDI-OH.

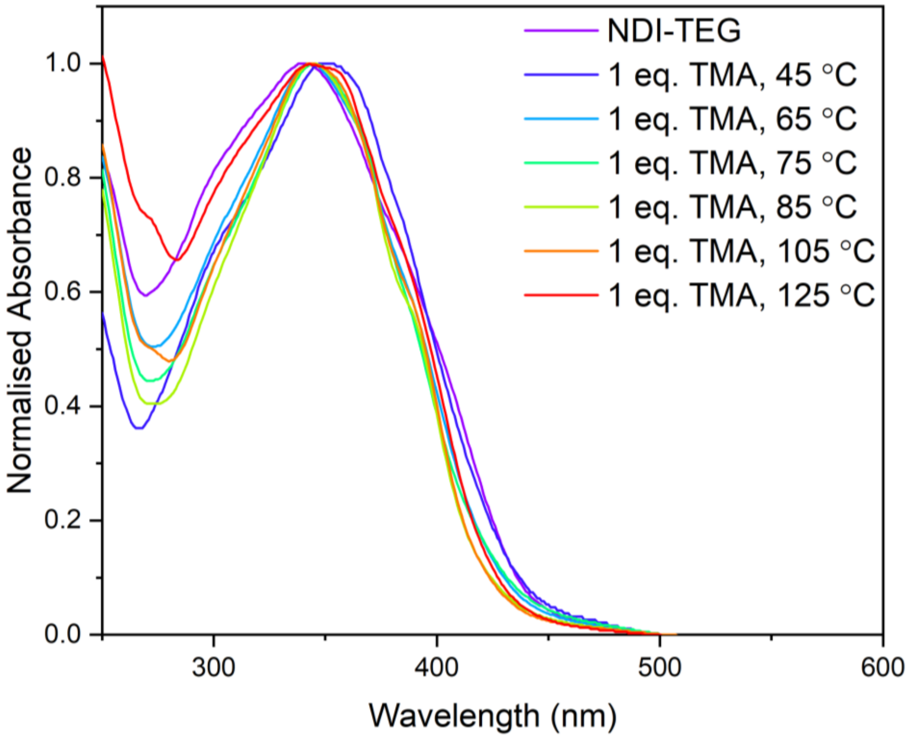

Figure S23. *UV-visible absorption spectra of NDI-TEG doped with 1 molar equivalent of TMA and drop-cast at temperatures between 45 °C and 125 °C.*

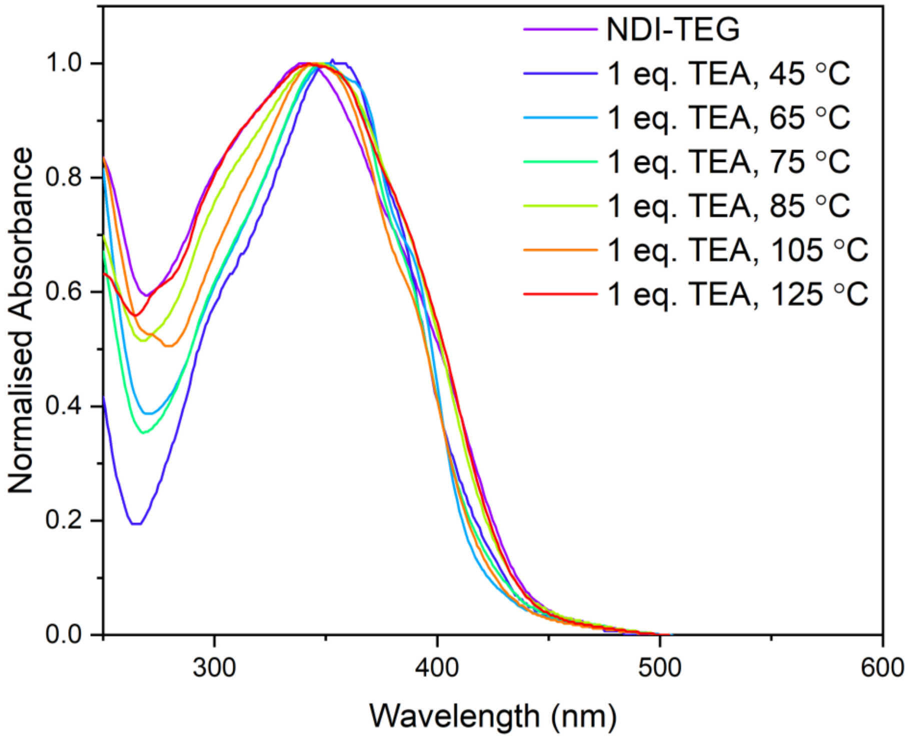

Figure S24. *UV-visible absorption spectra of NDI-TEG doped with 1 molar equivalent of TEA and drop-cast at temperatures between 45 °C and 125 °C.*

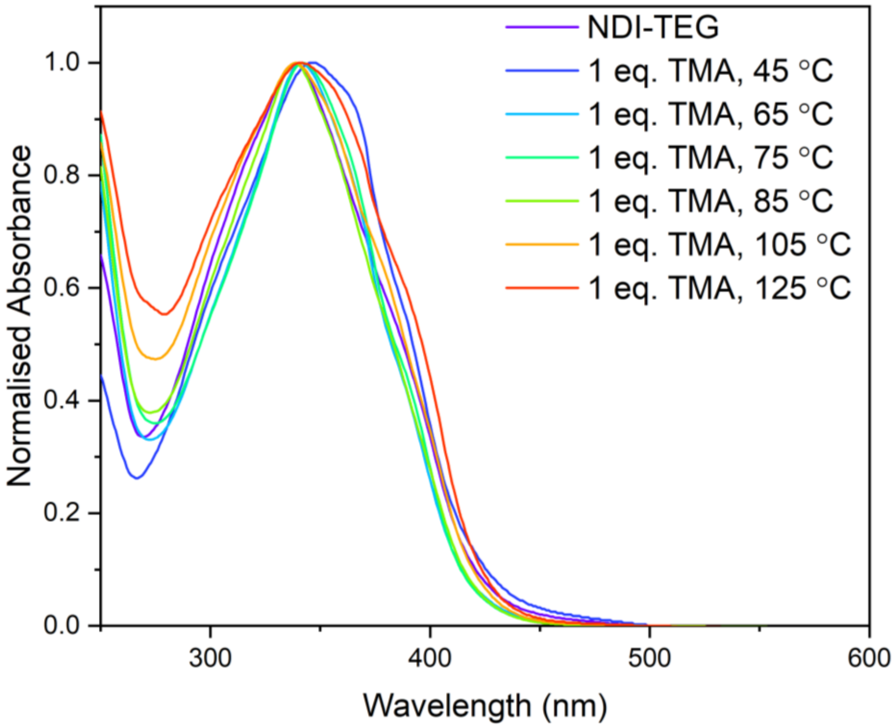

Figure S25. *UV-visible absorption spectra of NDI-TEG doped with 1 molar equivalent of TMA and drop-cast at temperatures between 45 °C and 125 °C. Solution of NDI-TEG was run through an ion-exchange column before doping.*

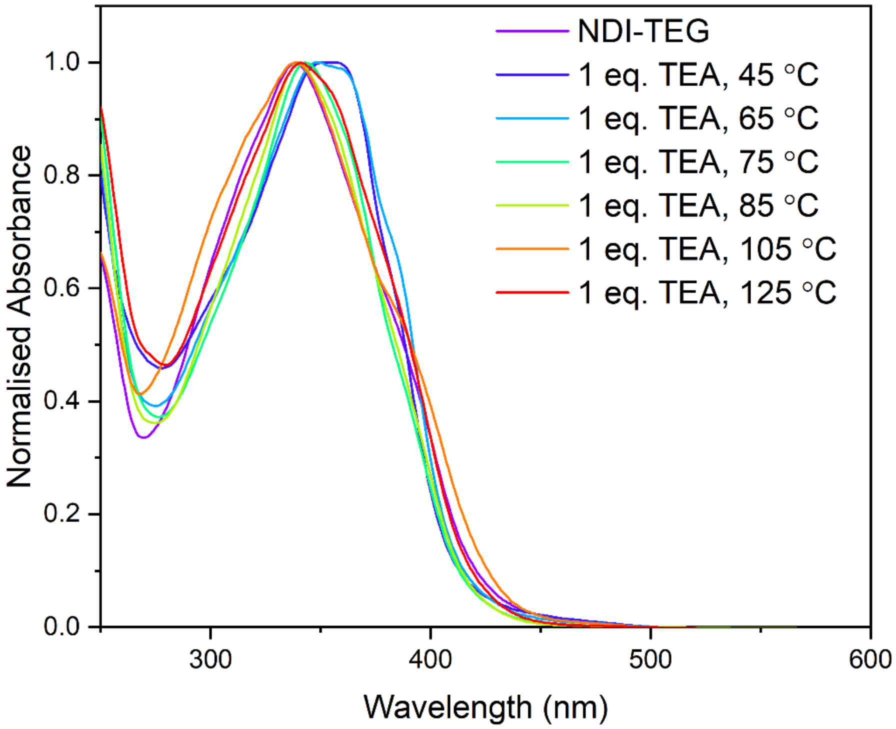

Figure S26. *UV-visible absorption spectra of NDI-TEG doped with 1 molar equivalent of TEA and drop-cast at temperatures between 45 °C and 125 °C. Solution of NDI-TEG was run through an ion-exchange column before doping.*

References:

1. Q. Sun, H. Wang, C. Yang and Y. Li, *Journal of Materials Chemistry*, 2003, **13**, 800-806.
2. J. Hou, Z. a. Tan, Y. Yan, Y. He, C. Yang and Y. Li, *Journal of the American Chemical Society*, 2006, **128**, 4911-4916.
3. Y. Li, *Organic Optoelectronic Materials*, 2015.
4. S. Stoll and A. Schweiger, *Journal of Magnetic Resonance*, 2006, **178**, 42-55.
5. S. De and S. Ramakrishnan, *Chemistry – An Asian Journal*, 2011, **6**, 149-156.
6. R. E. Dawson, A. Hennig, D. P. Weimann, D. Emery, V. Ravikumar, J. Montenegro, T. Takeuchi, S. Gabutti, M. Mayor, J. Mareda, C. A. Schalley and S. Matile, *Nature Chemistry*, 2010, **2**, 533-538.
7. M. Nakano, M. Sawamoto, M. Yuki and K. Takimiya, *Organic Letters*, 2016, **18**, 3770-3773.
8. J. Xu, B. Chen, J. Lv, D. Chang, D. Niu, S. Hu, X. Zhang, Z. Xin and L. Wang, *Dyes and Pigments*, 2019, **170**, 107559.
9. B. Russ, M. J. Robb, B. C. Popere, E. E. Perry, C.-K. Mai, S. L. Fronk, S. N. Patel, T. E. Mates, G. C. Bazan, J. J. Urban, M. L. Chabinyc, C. J. Hawker and R. A. Segalman, *Chemical Science*, 2016, **7**, 1914-1919.
10. Y. Matsunaga, K. Goto, K. Kubono, K. Sako and T. Shinmyozu, *Chemistry – A European Journal*, 2014, **20**, 7309-7316.
11. J. B. Edson, C. S. Macomber, B. S. Pivovar and J. M. Boncella, *Journal of Membrane Science*, 2012, **399-400**, 49-59.